ROBUST IMPLEMENTATION OF THE MODEL PREDICTIVE CONTROL FOR DC-DC POWER CONVERTERS AND INDUSTRIAL CONTROL APPLICATIONS

by

MOHAMED EMHEMED ALBIRA

A dissertation submitted in partial fulfillment of the
requirements for the degree of

DOCTOR OF PHLOSOFY IN ELECTRICAL AND COMPUTER ENGINEERING

2022

Oakland University
Rochester, Michigan

Doctoral Advisory Committee:

Mohamed Zohdy, Ph.D., Chair
Subramaniam Ganesan, Ph.D.
Gary Barber, Ph.D.
Li Li, Ph.D.

إهـــــــــــداء

بسم الله الرحمن الرحيم و الصلاة و السلام علي سيدنا محمد و علي أله و أصحابه أجمعين

أمــا بعـــــد,,,

إلي روح أبي الطيبة الطاهرة الزكية

إلي نبع الحنان أمي الغالية

إلي زوجتي الحبيبة و ابنائي

الي إخوتي و أخواتي الاعزاء

إلي كل أفراد أسرتي و أقاربي و أصدقائي و زملائي

إلي كل أساتذتي و كل من علمني ولو حرف

إلي دولتي ليبيا و إلي أمتي الاسلامية

لكم يا أحبتي أهدي هذا العمل المتواضع

نسأل الله سبحانه و تعالي أن يتقبله مني خالصا لوجهه الكريم

مع خالص الشكر

محمد البيرة

ACKNOWLEDGMENT

First, Glory be to our Lord, praise and thanks be to you a lot good and blessed. Oh God, praise and thanks be to you as it should be for the majesty of your face, the greatness of your authority, and the majesty of your place,

and blessing and peace be upon our prophet Mohammed, his family and his companions.

Second, I would like to acknowledge and give my warmest thanks to my advisor , Dr. Mohamed Zohdy who made this work possible. His guidance and advice carried me through all the stages of my PhD journey. I would also like to thank my committee members Dr. Subramaniam Ganesan, Dr. Li Li, and Dr. Gary Barber for letting my defense be an enjoyable moment, and for their brilliant comments and suggestions, thank you so much.

Also, I would also like to express special thanks and gratitude to my family, specifically my mother, my dear wife, brothers, sisters and my children; they were always supportive with encouragements and advice when I needed them.

Finally, Also, I would like to give warm thanks to my relatives, friends, and colleagues for their supports to achieve this goal.

Mohamed Emhemed Albira

ABSTRACT

ROBUST IMPLEMENTATION OF THE MODEL PREDICTIVE CONTROL (MPC) FOR DC-DC POWER CONVERTERS AND INDUSTRIAL CONTROL APPLICATIONS.

by

Mohamed Emhemed Albira

Advisor: Mohamed Zohdy, Ph.D.

This dissertation addresses the development of the robustness and strength of the Model Predictive Control algorithm subjected to input constraints for a plant system with and without parameters' uncertainties. In the beginning, the MPC control system was implemented for systems with no types of parameters' uncertainties. The proposed system models were stable and linear and all of its parameters were fully known. They were formulated in model state-space system format. The main objective of this control system design was to maintain a smooth and constant output signal that could easily track the assigned desired output signal. The technical process of this control design was to calculate the optimal solutions for the proposed plant system by optimizing the Quadratic programming problem (QP) subjected to linear inequality constraints. Therefore, the proposed control system successfully forced the outputs of the proposed systems to track the output reference signals in a fast response and with very small steady-state errors, even with the change in prediction horizon values.

The second control system approach was for a system model which assumed its parameters' uncertainties. In the other words, the parameters were not precisely known, but they were bounded in a minimum and maximum range. The parameters' uncertainties and the converter's switching behaviors made it act as a highly nonlinear system. Therefore, the Adaptive Model Predictive controller (AMPC) with the Linear Parameter Varying (LPV) control algorithm was implemented to address these issues and to secure a sustainable output signal with on types of noise or degradations. In this algorithm, the LPV model was created out of a set of Linear Time-Invariant (LTI) models, which are used to update the AMPC controller based on the feedback signals that come from the plant model and the change in the system parameters. Due to the changes in the plant model parameters over time, the AMPC was the perfect control approach due to its capability to update its prediction model and the operating condition over a prediction horizon interval. Since the AMPC is an online optimization-based approach, the QP variables and parameters can be tuned based on changes of the system measurements in real-time, and the LPV scheduling parameters. The proposed AMPC and LPV algorithm was compared against different control system approaches. Also, the proposed AMPC and LPV algorithm was implemented using an Arduino Mega 2560 microcontroller to show its performance in a real-time environment. In summary, from the outputs and the results, the proposed AMPC and LPV control system showed higher levels of the performance interims of the purified output, faster responses, and the computational time in both the simulation and real time results.

MATLAB, SIMULINK, and ARDUINO support packages were used for the system design and implementations.

TABLE OF CONTENTS

TABLE OF CONTENTS-Continued

TABLE OF CONTENTS-Continued

LIST OF TABLES

LIST OF FIGURES

CHAPTER ONE

INTRODUCTION

The base requirements of the control systems are concerned with the system's stability, dynamic behaviors, and robustness of the closed-loop system. Many control schemes have been extensively studied to work for the power converters and the industrial applications, such as the hysteresis control and linear control with the pulse width modulation [1]. In addition to the aforementioned control schemes, there are more efficient control systems such as Sliding Mode Control, Fuzzy Logic Control, and Model Predictive Control (MPC) systems. Although they are computationally complex, they can be implemented using the developed powerful microprocessors or field Programmable Gate Arrays (FPGA). These control systems are not only suitable for the bases mentioned above, but they show high robustness against the nonlinear behaviors caused by the switching nature of the power converters, the unknown values of the controlled system parameters, and the fast responses with high performance in terms of the control system regulations [2] and [3].

1.1 Fundamental and Background of Model Predictive Controller

Model Predictive Control (MPC) is an optimal control technique that uses the optimization at each sampling time Ts over a predicted decision interval Np to calculate the system's future optimal solution. MPC was first funded in the late 70s by Richalet et al., then get developed by Cutler and Ramaker for the oil and chemical process industries [4]. However, many applications currently use MPC to control their functionalities. MPC has also named a receding horizon control and, in some references, calls it Quadratic

Programming Control (QPC) and Optimization and Prediction Control (OPC) [4]. MPC has significantly improved in terms of the academic research against the traditional feedback controllers such as the Proportional Integrals Derivatives (PID), sliding mode, and state feedback control systems [40]. Figure (1) shows the growth of the four mentioned controllers in the period between 1960 to 2010. In the beginning, MPC had not yet gotten any attention until about 2003 when it grew the highest interest from many researchers and book authors. On the other hand, the above-mentioned conventional control systems lagged behind because they were not effectively valid in handling applications with high levels of uncertainties and computational complexities systems with the satisfaction of a set of constraints [4]-[6].

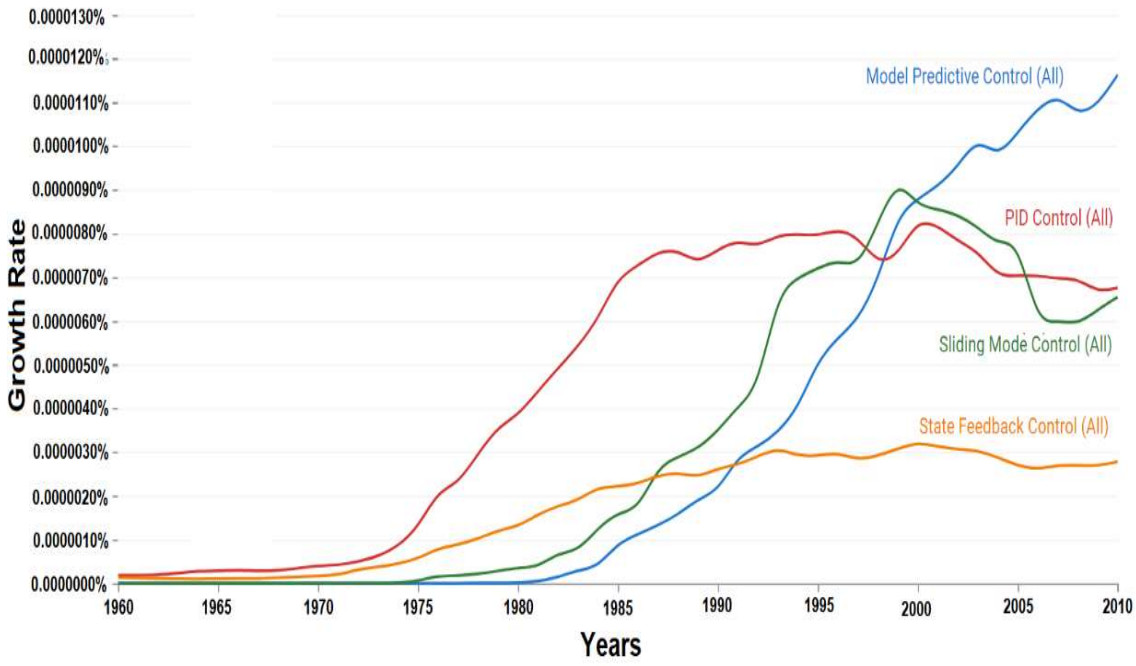

Fig. 1.1 the Ngrams search for the MPC against the traditional controllers

The MPC controller's advantages are that it can handle multi-input-multi-output (MIMO) systems with small changes in the formulation compared to the single-input-single-output (SISO) systems and its flexible structure in the event of errors. Another advantage is that the MPC control system is subjected to handle input, states, and output constraints, which many control theories have failed to handle.

1.2 MPC Strategy and Methodology

The MPC control system predicts the system outputs y at each sampling time Ts for a defined prediction horizon interval Np, as is shown in Figure 2 [39]. The predicted output $y(k+i|k)$ for $i = 1,2,\dots,Np$ is based on the past and current information collected from the system output in the past and up to the current instant time k. The optimal control signals are calculated by optimizing the objective function or the cost function in some references (1). This is to force the system output to keep tracking the assigned reference signal $r(k+i|k)$. There are different forms of the objective cost function that are used to minimize the error amounts between the predicted system outputs and the assigned reference trajectory $r(k)$; the most common ones are Linear

Programming (LP), and Quadratic Programming (QP) functions, which will be used in the MPC design in this dissertation. The general format of the QP cost function for the predicted state trajectory $x(k)$, in terms of the input control signal $u(k)$ subjected to an inequality constraint, is illustrated in the formula below.

$$J(x(k),u(k))\sum_{k=0}^{Np-1}(\|x(k+i)\|^2 Q+\|u(k+i)\|^2 R)+\|x(k+i)\|^2\overline{Q} \quad \text{subj. to} \quad x(k)=Ax(k)+Bu(k) \quad i=0,1,2\dots Np \tag{1}$$

Where the k is the discrete time period, the J is the cost based on the system state $x(k)$ and control input $u(k)$. The weights Q and R are used to adjust the influences of the

error in the output and the input respectively. And in case of calculating the cost J over an infinite prediction, that requires to choose an appropriate value for weighting matrix $\overline{Q}$ [4] - [7] and [36] [37].

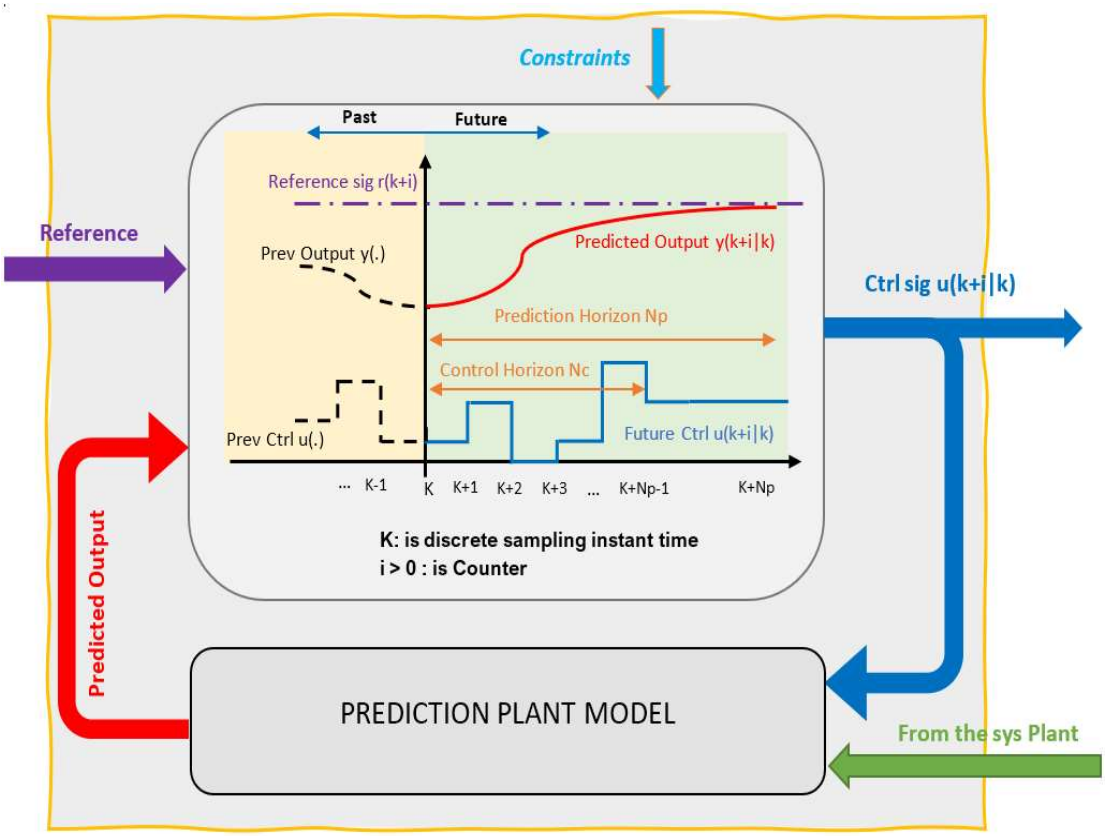

Fig.2 MPC strategy

1.3 Literature Review

The power of modern control systems is their capability to carry out the significant issues that the power electronics dc-dc converters and the industrial

applications overcome, such as the nature of bilinear characteristics, non-minimum phase behaviors, and parameters' uncertainties [7] and [8]. These issues are highly complex when it comes to the control system design. Many control strategies have been studied in depth to carry out these problems and enhance the power electronics and applications' work performance. Various MPC algorithms have been developed during the last few decades to work for power electronics and the industrial applications. In some studies, the Finite Control Set (FCS-MPC) and the Current Control Set (CCS-MPC) have been deeply studied as in the references [7]-[11]. Other researchers have developed different ways to enhance the online optimization to solve the Quadratic Programming (QP) in a shorter time [12]-[20].

The authors in [8] investigated the CCS-MPC control system to address the non-minimum phase behavior that the boost converter overcomes. The strategy also considers reducing the computational burden by reducing the number of prediction horizon intervals. This control algorithm works well with both of the dc-dc converters' working modes, the continuous condition mode (CCM) and the discontinuous condition mode (DCM). However, it requires an observer algorithm to maintain accurate reference tracking and better estimate the system parameters' mismatches. The reference [10] studied the advantages of using the FCS-MPC control system for a coupled-inductor buck-boost converter to improve the current tracking and reduce the converter's power losses. Their proposed FCS-MPC algorithm works well to regulate the operations of the buck-boost converter in buck and boost modes, and it shows a reasonable enhancement in terms of the power losses. In the reference [11], an offset-free finite set control-MPC controller (OFFCS-MPC) and higher-order sliding mode observer (HOSO) have been

implemented for dc-dc buck converter feeding constant power loads (CPL) with unknown load variations and parameter's uncertainties. Although the OFFCS-MPC performed very robustly controlling the dc-dc buck converter, the resultant high computational burden requires higher speed and bigger memory in terms of hardware; it is also not suitable to work for bilinear converters such as boost or buck-boost dc-dc power converters. The optimal constrained MPC control system was solved offline based on the piecewise affine (PWA) method to approximate the prediction model for the proposed dc-dc boost converter [12]. The MPC control system implementation in [13] was based on the PWA system modeling, which successfully captured the hybrid and the switching behaviors of the dc-dc buck converter. When the parameters' uncertainties and the nature switch behaviors in a system like the power converters, a technique called Linear Parameters Varying (LPV) could take place where the system could be linearized and stabilized around different operating conditions. Then, the linearized system models were used as the prediction model fed to the MPC controller based on the changes in the system output. Other MPC control schemes were implemented for LPV systems using the quasi-min-max algorithm; this algorithm depended on a robust state observer and the linear matrix inequality (LMI) [15]-[18], [25]. On a technical note [19], the Adaptive MPC (AMPC) control strategy was implemented for systems with parametric uncertainties. The AMPC control system was built based on the min-max optimization principle. The min-max strategy is the way to estimate the system parametric uncertainties and to get the estimated error converges. Although this algorithm has succeeded in estimating the system parameters' uncertainties, it struggles to address the constraints over the system states or the outputs.

1.4 Motivation and Research Goal

From the literature review, it is obvious that both the MPC and the AMPC-LPV control algorithms have appeared as promising control methods that successfully work in the field of the dc-dc power converters and the industrial applications. The key motivations behind this success are its flexibility, robustness, and its ability to be implemented using the integrated circuit such as the FPGA [14], and [25] or on a modern microcontroller, such as the Arduino Mega 2560.

The literature has demonstrated that many MPC schemes have solved the base problems, such as the non-minimum phase dynamics, and the nature behaviors of the switching modes using the CCS-MPC and FCS-MPC control algorithms [8]-[10]. Others have shown the variety of faster optimization algorithms [11] - [20]. Although the above-mentioned algorithms are highly effective, not all of them applied constraints. Others did not consider all the system parameters' uncertainties. Furthermore, real-time implementation was not considered in terms of the efficiency and the cost. Therefore, one can see that the gaps in the research leave much to be considered.

Motivated by previously discussed research, the goal of this dissertation was to study in-depth the effectiveness of the constrained MPC control system on different types of dc-dc power converters and industrial applications in the presence of the above-mentioned problems, such as the non-minimum phase dynamics, the behaviors of the switching modes, and the additive input disturbances. In addition, the AMPC with LPV control algorithm for the system parameters' uncertainty of power converters were studied. The AMPC with LPV control algorithm was designed to work with any of the non-isolated dc-dc power converters, such as the buck, boost, and buck-boost converters

considering the non-minimum phase dynamics, the behaviors of the switching modes, and the system parameters' uncertainties. Also, this proposed algorithm was tested in real-time implementation to ensure simplicity in terms of the computational burden and high efficiency in terms of the system output quality.

1.5 The Dissertation Contributions

This dissertation aimed to deeply study the theoretical analysis and practical implementations of the MPC control algorithms for dc-dc power converters and the industrial applications.

In the beginning, two case studies were proposed. The first one assumed that the proposed system plant was fixed, and no external disturbance was applied to the system model. The second case study assumed there was an input disturbance added to the proposed system model. Then, in a separate chapter, another study was conducted of a system model with problems of the converter's switching behaviors and the parameters' uncertainties. A summary of the main contributions are listed below:

- Linear MPC control system was designed based on the quadratic programming optimization process with inequality constraints applied to the input control signal for tow system models, with the assumptions that they were:
  - Designed with all the parameters fixed and known.
  - Formulated using the averaged model state space system.
  - Ill of the non-minimum phase dynamic problem.
  - Effected by the input disturbances in the second case study.
  - Mathematically stable and linear.

- Tested to see the effectiveness of the changes in prediction horizon values on the system outputs and the control responses.

➢ The AMPC and LPV control algorithm was implemented to control a dc-dc buck-boost converter which was:

- Designed assuming that the uncertainty parameters were not precisely known, but they were bounded in a min-max range.
- Linearized at different operating conditions to perform a set of LTI models; those models defined a Linear Parameter-Varying (LPV) model.
- Constrained to limit the amplitude of the input control signal within a boundary of 0 and highest value of the duty cycle.
- Tested at different prediction horizons to measure performance.
- Implemented in real time using Arduino Mega 2560 microcontroller and worked well to provide the desired output voltage at different levels and in faster response.

This dissertation was constructed in five chapters. Chapter One covers the proposed control system and the proposed case studies introductory, the fundamentals and the history of the predictive control systems, the literature review, the motivations, and the contributions. In Chapter Two, the analysis and work dynamics of the proposed system models and their linearization process are discussed. Chapter Three looks at the theory and the algorithms that are used to implement the MPC control system for linear systems such as the proposed dc-dc buck-boost converter and the buck convert driven dc-motor. Chapter Four presents the implementations of the AMPC and LPV control system for a dc-dc buck-boost converter system model whose parameters have some degree of

uncertainties; it includes how the AMPC and LPV control algorithm get updated to cover the parameters' uncertainties problem. Also in this chapter, the proposed AMPC with LPV control system was implemented in real-time using the Arduino Mega 2560 microcontroller. The proposed control system results and outputs were compared with different control system approaches in the literature. The conclusion and the future works were presented in Chapter Five.

CHAPTER TWO

THE DYNAMIC SYSTEM MODELING AND DESIGN

The first step towards accurate system design is to carefully consider most of the details that represent the real-time system. Mathematical modeling is the way to approximate the physical system dynamics [21]. The precise system outputs and results come when the differences, or the error between the mathematical modeling and the real physical system, are minimized. The following sections are focused on illustrating the mathematical models of the proposed dc-dc converters and the industrial applications.

2.1 dc-dc Power Converters

In today's modern electronics devices, the direct current (dc-dc) power converters are important components for numerous devices. These converters work to convert the amplitude of the power from a level to another level. The three most significant dc-dc power converters are the step down buck, step up boost, and the step up and step down buck-boost dc -dc converters. In this subsection, the dc-dc buck-boost converter is the proposed system that will be studied and analyzed in detail.

2.2 The dc-dc Buck-Boost Converter:

The dc-dc buck-boost converter is a non-isolated dc-dc converter which works to step up and step down the output power. In this type of the dc-dc converters, the energy storage elements (the inductors and capacitors) and the switching components (the metal–oxide–semiconductor field-effect transistor (MOSFET)) are playing significant roles in its working behaviors. To this end, the mathematical modeling is derived to simplify the complexity of this converter's electronics circuit. Due to the switching behaviors of the

MOSFET and the Diode, the proposed dc-dc converter acts in two modes: ON mode and OFF mode. The ON mode when the switch is ON (sw = 1) closed for d ∗ Ts period of time and when the switch is OFF (sw = 0) opened for (1 − d)∗ Ts period of time. Where the d and *T*s are the duty ratio and the sampling time period respectively [22], [23] and [25]. Applying the Kirchhoff's voltage and current law to the converter's schematic circuit in Fig. 3 to illustrate the inductor current iL and output voltage vC. It should be noted that in this dissertation, the proposed dc-dc buck-boost converter considered working in a Continuous Condition Mode (CCM), which means that the inductor current always remained bigger than zero ($iL > 0$) [22] and [24]. The parameters in the circuit diagram are the VG for the input voltage, the SW represents the switching behavior of the MOSFET, L for the inductor, **dio** for the diode, C for the capacitor, rC and rL for the capacitor and inductor resistors, R for the resistive load [23].

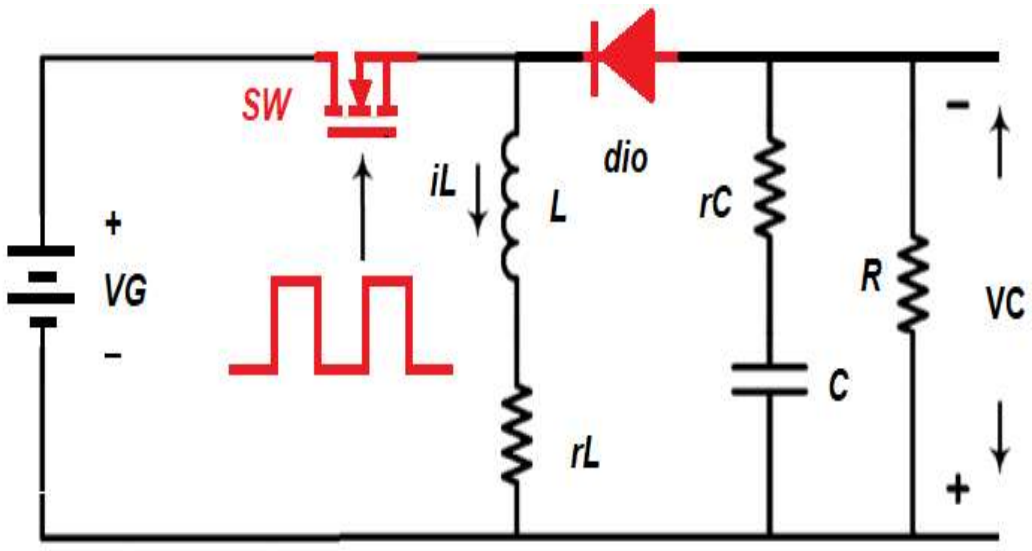

Fig. 2.1 the DC-DC buck-boost converter schematic Circuit

when the switch is ON: $0 < t < d * T$, the state space equation at the $sw = 1$ is given as

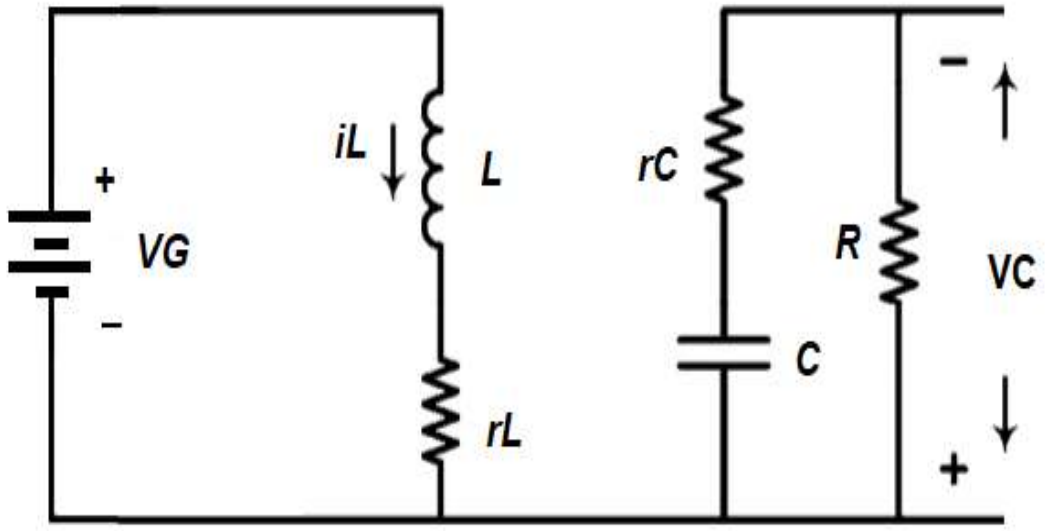

Fig.2.2 the dc-dc Buck-Boost Converter is in the ON mode (sw=1)

$$\frac{di_L}{dt} = \frac{-rC}{L} iL + \frac{1}{L} VG \tag{2.9}$$

$$\frac{dvc}{dt} = -\frac{1}{C*(R+rC)} vc \tag{2.10}$$

In form of the state space system the above differential equations can be illustrated as follows [21]-[27]:

$$\begin{aligned} \dot{x} &= A_1 x + B_1 u \\ y &= C_1 x \end{aligned} \tag{2.11}$$

$$A_1 = \begin{pmatrix} \frac{-rC}{L} & 0 \\ 0 & -\frac{1}{C*(R+rC)} \end{pmatrix}$$
$$B_1 = \begin{pmatrix} \frac{VG}{L} \\ 0 \end{pmatrix} \quad (2.12)$$
$$C_1 = [0\ 1]$$
$$D_1 = [0]$$

And when the switch is OFF: $d * T < t < T$, the state space equation $sw = 0$ is given as

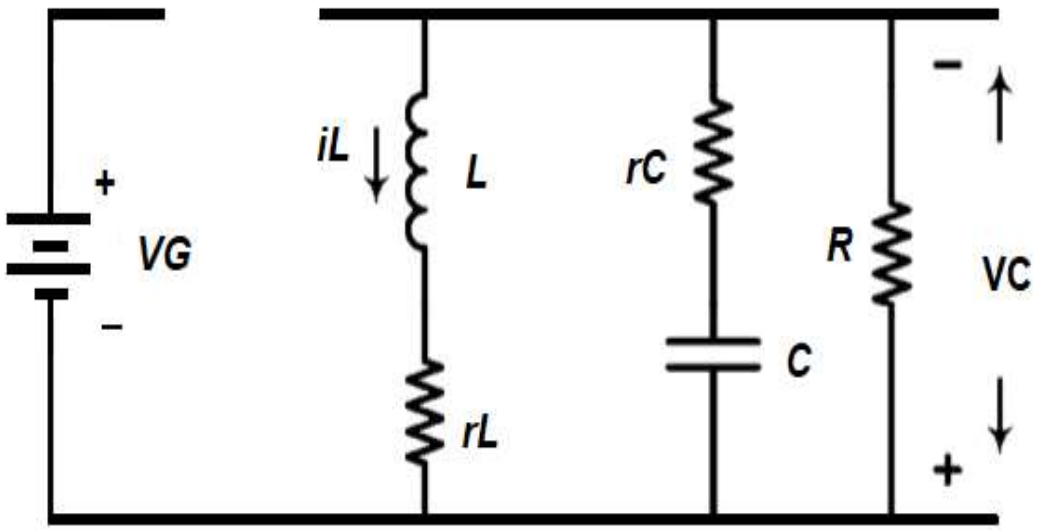

Fig.2.3 the dc-dc Buck-Boost Converter is in the OFF mode (sw=0)

$$\frac{diL}{dt} = -\left(\frac{R*rC+R*rL+rC*rL}{(R+rC)*L}\right) * iL + \left(\frac{-R}{(R+rC)*L}\right) * vc \quad (2.13)$$

$$\frac{dvc}{dt} = \left(\frac{R}{(R+rC)*C}\right) * iL - \left(\frac{1}{(R+rC)*C}\right) * vc \quad (2.14)$$

$$\dot{x} = A_2x + B_2u$$
$$y = C_2x \quad (2.15)$$

$$A_2 = \begin{pmatrix} -\left(\frac{R*rC+R*rL+rC*rL}{(R+rC)*L}\right) & \left(\frac{-R}{(R+rC)*L}\right) \\ \left(\frac{R}{(R+rC)*C}\right) & -\left(\frac{1}{(R+rC)*C}\right) \end{pmatrix}$$
$$B_2 = \begin{pmatrix} 0 \\ 0 \end{pmatrix}, \quad C_2 = [0\ 1], \quad D_2 = [0] \tag{2.16}$$

Where the system states $x = \begin{pmatrix} iL \\ vC \end{pmatrix}$ and the control signal $u = d$ duty cycle. For the purpose of the control system design the averaged model will be derived with consideration of duration of one switching period using the expression below [21]-[27].

$$\dot{x} = A_{avr}\, x + B_{avr}\, u \qquad \begin{cases} A_{avr} = d * A_1 + (1-d) * A_2 \\ B_{avr} = d * B_1 + (1-d) * B_2 \\ C_{avr} = d * C_1 + (1-d) * C_2 \\ D_{avr} = d * D_1 + (1-d) * D_2 \end{cases} \tag{2.17}$$
$$y = C_{avr}\, x + D_{avr}\, u$$

By substituting the expressions (2.9) to (2.16) with the expression (2.17) the averaged model can be illustrated as follow [21]-[27]

$$\frac{diL(t)}{dt} = \left(-\frac{-rL(R+rC)-(R*rC)(1-d)}{L(R+rC)}\right) iL(t) - \left(\frac{R(1-d)}{L(R+rC)}\right) vC(t) + \left(\frac{-d}{L}\right) vG(t)$$
$$\frac{dvC(t)}{dt} = \left(\frac{R(1-d)}{C(R+rC)}\right) iL(t) - \left(\frac{1}{C(R+rC)}\right) vC(t) \tag{2.18}$$

And in the form of state space system as bellow

$$A_{avr} = \begin{pmatrix} -\left(\frac{-rL(R+rC)-(R*rC)(1-d)}{L(R+rC)}\right) & -\frac{R(1-d)}{L(R+rC)} \\ \frac{R(1-d)}{C(R+rC)} & -\frac{1}{C(R+rC)} \end{pmatrix}$$
$$B_{avr} = \begin{pmatrix} \frac{-VG*d}{L} \\ 0 \end{pmatrix} \tag{2.19}$$
$$C_{avr} = [0 \quad 1], \quad D_{avr} = [0]$$

2.3 The dc-dc Buck-Boost Linearization Process

The illustrated differential equations in the expression (2.18) represents the averaged model of the proposed dc-dc buck-boost converter, which are used to illustrate the continuance time averaged inductor current $iL(t)$ and the capacitor voltage $vC(t)$.

Obviously, from equations (2.18), the system is nonlinear due to the multiplication terms of the time-varying quantities of the inductor current $\mathrm{iL(t)}$, capacitor voltage $\mathrm{vC(t)}$, and the input voltage $\mathrm{vG(t)}$ with the duty cycle d. Therefore, given the aim of linear control design, this nonlinear behavior must be linearized around equilibrium points. After a given number of sampling periods, the converter reaches the steady state conditions. This means that the duty cycle $\mathrm{d} = \mathrm{D}$ and the input voltage $\mathrm{vG(t)} = \mathrm{VG}$ reach the constant values, applying the inductor-volt second balance and the capacitor charge balance principles as well as the small-ripple approximations, to illustrate the steady state or (DC values) of the inductor current and the capacitor voltage values.

$$\mathrm{IL} = -\frac{\mathrm{VC}}{(1-\mathrm{D})\mathrm{R}} \ , \quad \mathrm{VC} = -\frac{\mathrm{D}}{(1-\mathrm{D})}\mathrm{VG} \ , \quad \mathrm{D} = \frac{\mathrm{VC}}{\mathrm{VC}+\mathrm{V}} \tag{2.20}$$

Since the expressions in (2.20) are at the steady state conditions (constant DC values), their derivatives will be zero. To derive the small-signal ac model that perturbs around the steady state operating points of the IL and VC, the input voltage $\mathrm{vG(t)}$ and the duty cycle d will be assumed to be equal to the values at the steady state operating points of the given VG, D and the perturbations added to them, as they represented with the hat on them ($\tilde{\cdot}$) [22],[24], and [26].

$$\begin{aligned} &\mathrm{vG(t)} = \mathrm{VG} + \widetilde{\mathrm{vG}}(\mathrm{t}), \quad \mathrm{d(t)} = \mathrm{D} + \tilde{\mathrm{d}}, \quad \mathrm{iL(t)} = \mathrm{IL} + \widetilde{\imath\mathrm{L}} \\ &\mathrm{vC(t)} = \mathrm{VC} + \widetilde{\mathrm{vC}}, \end{aligned} \tag{2.21}$$

Note that the ac small perturbations ($\tilde{\cdot}$) are much smaller than the steady-state values considered in the averaged model in equations (2.18). The linearized system is performed by separating the ac small signals from the steady-states variables. Then, the linearized dynamic model can be represented as a continuous-time state-space system, as in the expression below:

$$\tilde{x} = A_{lin} * x + B_{u,lin} * u$$
$$y = C_{lin} * x \tag{2.22}$$

$$A_{lin} = \begin{pmatrix} -\frac{(-rL)(R+rC)-(R*rC))D'}{L(R+rC)} & -\frac{RD}{L(R+rC)} \\ \frac{RD}{C(R+rC)} & \frac{-1}{C(R+rC)} \end{pmatrix},$$
$$B_{u,lin} = \begin{pmatrix} \frac{VG}{L} \\ 0 \end{pmatrix} \tag{2.23}$$
$$C_{lin} = (0 \quad 1), \quad D_{lin} = 0$$

Where the $A_{lin}, B_{lin}, C_{lin}$ and D_{lin} are the system state, input, output state and output noise matrices. The system state $\tilde{x} = [\widetilde{iL}\ \widetilde{vC}]^T$ represents the inductor current and the capacitor voltage. The system input $\tilde{u} = \tilde{d}$ are the ac small signal duty cycle (the control input signal), the $y = VC$ is the system output, the term $D' = 1 - D$, and the expression $(.)^T$ indicates the transposition of a vector or a matrix [22]-[27].

2.4 dc-dc Buck Converter Driving dc-Motor System Design

A direct current dc-motor is one of the main components when it comes to the high precision motion systems. Its accuracy made it extensively required in many industrial instruments, tools, and devices. Many applications use the dc-motor for their motion operations. For instance, small applications such as toys, and large applications such as electric vehicles, elevators, and hoists [28].

To adjust the speed and to increase the permission of the dc-motor, various control systems are used to regulate the armature current and voltage. One of the simplest and most commonly used controlling methods is the Pulse-Width Modulation (PWM) technique. The PWM technique works well but the nonlinearity of the pulse switching can cause a rough start of the motor and variations in the armature voltage and current, which could damage the DC-motor mechanism by placing too much stress on the

electronic components of the DC-motor circuitry [28]-[30]. The dc-dc buck, boost, and buck-boost converters are effective solutions for these types of problems because they contain the energy-storage components (e.g., inductor and capacitor) which are capable of generating the required noiseless voltage and current to start the dc-motor smoothly. Combining dc-dc converters with dc-motors also can improve the velocity tracking performance of the dc-motor by providing purified output voltage and current to the dc-motor [31] and [32]. To this end, a dc-dc buck converter is the proposed tool to supply the dc-motor with a regulated dc current and voltage [31].

2.4.1 dc-dc Buck Converter And dc-Motor Mathematical Modeling

The proposed model of the dc-dc buck converter driven dc-motor circuit shown in the Fig. 4 contains two parts, the generic PWM-based dc-dc buck converter, and the permanent magnet dc-motor. The first part of the circuit describes: the parameters r_S for the internal resistance of the source, La for converter inductor, r_L for internal resistance of the inductor, Cr for the converter capacitor, the duty cycle δ, Vin for the voltage source, and Ts is the sampling time period. The parameters for the second part are: L_m is the motor inductor, the Rm is the armature winding resistance, ke is the counter electromotive force constant, k_m is the motor torque constant, J_0 is the moment of inertia, B is the motor viscous friction coefficient, T_L is the load torque [33].

Applying the Kirchhoff's voltage and current laws (KVL, KCL) and the Newton's law to the circuit shown in Fig. 2, the mathematical model can be derived to illustrate the inductor current i_L, capacitor voltage vo, the armature current im, and the angular velocity w_m [33].

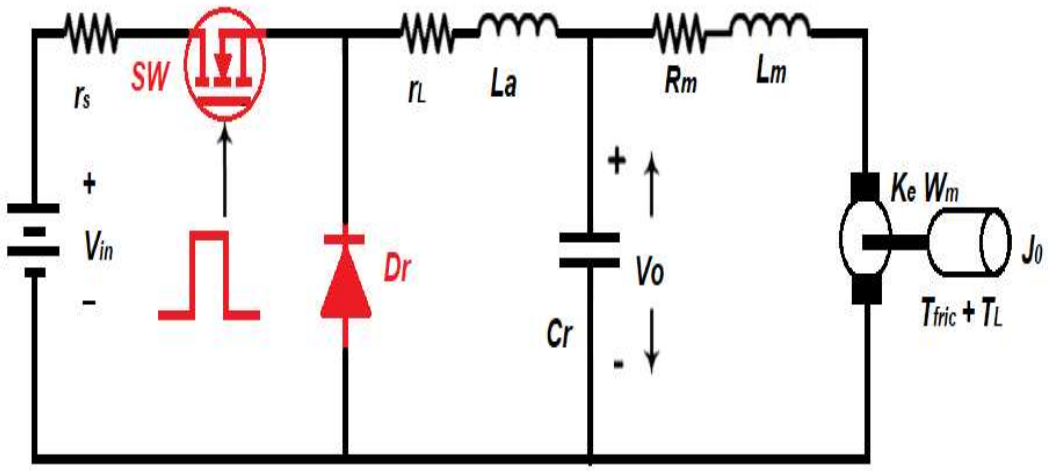

Fig. 2.4 the dc-dc buck converter/dc-motor schematic circuit

Based on the buck converter switching behavior, the system will be responded into two subsystems that are numerated 1 when the switch is on, and 0 when the switch is off. The obtained dynamic system equations for the proposed system as follow:

- The System represented when the $\mathrm{sw} = 1$ (on)

$$\frac{\mathrm{diL}}{\mathrm{dt}} = -\frac{(\mathrm{rL})}{\mathrm{La}}\mathrm{iL} - \frac{1}{\mathrm{La}}\mathrm{vC} + \frac{1}{\mathrm{La}}\mathrm{Vn} \tag{2.24}$$

$$\frac{\mathrm{dvc}}{\mathrm{dt}} = \frac{1}{\mathrm{Cr}}\mathrm{iL} - \frac{1}{\mathrm{Cr}}\mathrm{im} \tag{2.25}$$

$$\frac{\mathrm{dim}}{\mathrm{dt}} = \frac{1}{\mathrm{Lm}}\mathrm{vC} - \frac{\mathrm{Rm}}{\mathrm{Lm}}\mathrm{im} - \frac{\mathrm{ke}}{\mathrm{Lm}}\mathrm{w_m} \tag{2.26}$$

$$\frac{\mathrm{dw_m}}{\mathrm{dt}} = \frac{\mathrm{km}}{\mathrm{J_0}}\mathrm{im} - \frac{\mathrm{B}}{\mathrm{J_0}}\mathrm{w_m} - \frac{\mathrm{T_L}}{\mathrm{J_0}} \tag{2.27}$$

Which can be represented in a state space as follows

$$\dot{\mathrm{x}} = \mathrm{A1} * \mathrm{x} + \mathrm{B1} * \mathrm{u} + \mathrm{B2_d} * \mathrm{dis}$$
$$\mathrm{y} = \mathrm{C1} * \mathrm{x} \tag{2.28}$$

$$A1 = \begin{pmatrix} -\frac{rL}{La} & -\frac{1}{La} & 0 & 0 \\ \frac{1}{Cr} & 0 & \frac{-1}{Cr} & 0 \\ 0 & \frac{1}{Lm} & -\frac{Rm}{Lm} & -\frac{ke}{Lm} \\ 0 & 0 & \frac{-km}{J_o} & \frac{-B}{J_o} \end{pmatrix}, \quad B1 = \begin{pmatrix} \frac{Vin}{La} \\ 0 \\ 0 \\ 0 \end{pmatrix}, \; B2_d = \begin{pmatrix} 0 \\ 0 \\ 0 \\ -\frac{T_L}{J_o} \end{pmatrix} \tag{2.29}$$

$$C1 = (0 \quad 0 \quad 0 \quad 1) \qquad D1 = \begin{pmatrix} 0 \\ 0 \\ 0 \\ 0 \end{pmatrix}$$

- The System represented when the $sw = 0$ (off)

$$\frac{diL}{dt} = -\frac{rL}{La} iL - \frac{1}{La} vc \tag{2.30}$$

$$\frac{dvc}{dt} = \frac{1}{Cr} iL - \frac{1}{Cr} im \tag{2.31}$$

$$\frac{dim}{dt} = \frac{1}{Lm} vc - \frac{Rm}{Lm} im - \frac{ke}{Lm} * w_m \tag{2.32}$$

$$\frac{dw_m}{dt} = \frac{km}{J_o} im - \frac{B}{J_o} * w_m - \frac{T_L}{J_o} \tag{2.33}$$

And the state space representation for the mode can be expressed as follows

$$\begin{aligned} \dot{x} &= A2 * x + B2 * u + B2_d * dis \\ y &= C2 * x \end{aligned} \tag{2.34}$$

$$A2 = \begin{pmatrix} -\frac{rL}{La} & -\frac{1}{La} & 0 & 0 \\ \frac{1}{Cr} & 0 & \frac{-1}{Cr} & 0 \\ 0 & -\frac{1}{Lm} & -\frac{Ra}{Lm} & -\frac{ke}{Lm} \\ 0 & 0 & \frac{-km}{J_o} & \frac{-B}{J_o} \end{pmatrix}, \quad B_u2 = \begin{pmatrix} 0 \\ 0 \\ 0 \\ 0 \end{pmatrix}, B2_d = \begin{pmatrix} 0 \\ 0 \\ 0 \\ -\frac{T_L}{J_o} \end{pmatrix} \tag{2.35}$$

$$C2 = (0 \quad 0 \quad 0 \quad 1), \qquad D2 = \begin{pmatrix} 0 \\ 0 \\ 0 \\ 0 \end{pmatrix}$$

Where the system state $x = [iL, vc, iM, w_m]^T$, the control signal is the duty cycle u and the dis is representing the input disturbance, and y is the system output.

2.4.2 dc-dc Buck Converter dc-Motor Averaged System Modeling

Due to the switching behavior, the averaged model can be expressed by adding the corresponding state space systems (2.28) and (2.34) and multiplying them with the duration of one switching period (duty cycle δ) to calculate the approximate state space averaged system, as in the equation (2. 36) [33].

$$\begin{aligned} \mathrm{A_{avr}} &= \mathrm{A1} * \delta + \mathrm{A2} * (1-\delta) \\ \mathrm{B_{u,avr}} &= \mathrm{B1} * \delta + \mathrm{B2} * (1-\delta) \\ \mathrm{B_{d,avr}} &= \mathrm{B1_d} * \delta + \mathrm{B2_d} * (1-\delta) \\ \mathrm{C_{avr}} &= \mathrm{C1} * \delta + \mathrm{C2} * (1-\delta) \\ \mathrm{D_{avr}} &= \mathrm{D1} * \delta + \mathrm{D2} * (1-\delta) \end{aligned} \tag{2.36}$$

Therefore, the averaged state matrices can be displayed as shown in equation below:

$$\mathrm{A_{avr}} = \begin{pmatrix} -\frac{\mathrm{rL}}{\mathrm{La}} & \frac{-1}{\mathrm{La}} & 0 & 0 \\ \frac{1}{\mathrm{Cr}} & 0 & -\frac{1}{\mathrm{Cr}} & 0 \\ 0 & -\frac{1}{\mathrm{Lm}} & -\frac{\mathrm{Rm}}{\mathrm{Lm}} & -\frac{\mathrm{ke}}{\mathrm{Lm}} \\ 0 & 0 & -\frac{\mathrm{km}}{\mathrm{J0}} & -\frac{\mathrm{B*Ra}}{\mathrm{J0}} \end{pmatrix}$$

$$\mathrm{B_{u,avr}} = \begin{pmatrix} \frac{\mathrm{Vin}}{\mathrm{La}} \\ 0 \\ 0 \\ 0 \end{pmatrix}, \qquad \mathrm{B_{d,con}} = \begin{pmatrix} 0 \\ 0 \\ 0 \\ \frac{-\mathrm{Tl}}{\mathrm{J_0}} \end{pmatrix} \tag{2.37}$$

$$\mathrm{C_{avr}} = (0 \quad 0 \quad 0 \quad 1), \qquad \mathrm{D_{avr}} = \begin{pmatrix} 0 \\ 0 \\ 0 \\ 0 \end{pmatrix}$$

2.4.3 dc-dc Buck Converter dc-Motor Linearization Process

By applying the small signal linearization technique and assuming that no saturation effects occur in the motor coil (the inductance La), the proposed dc-dc buck

converter combined with the dc-motor system model is linearized and it can be represented in a linear state space, as noted below:

$$\tilde{x} = A_{lin} * x + B_{u,lin} * u + B_{d,lin} * dis$$
$$y = C_{lin} * x \tag{2.38}$$

$$A_{lin} = \begin{pmatrix} -\frac{rL}{La} & \frac{1}{La} & 0 & 0 \\ \frac{1}{Cr} & 0 & -\frac{1}{Cr} & 0 \\ 0 & -\frac{1}{Lm} & -\frac{Rm}{Lm} & -\frac{ke}{Lm} \\ 0 & 0 & -\frac{km}{J0} & -\frac{B}{J0} \end{pmatrix}$$
$$B_{u,lin} = \begin{pmatrix} \frac{Vin}{La} \\ 0 \\ 0 \\ 0 \end{pmatrix}, \; B_{d,lin} = \begin{pmatrix} 0 \\ 0 \\ 0 \\ \frac{-Tl}{J_0} \end{pmatrix} \tag{2.39}$$
$$C_{lin} = (0 \quad 0 \quad 0 \quad 1), \; D_{lin} = (0)_{4\times 2}$$

Where the state $x = [iL, vC, \; iM, \; w_m]^T$ are for the converter inductor current, the converter capacitor voltage, the DC-motor armature current, and the system speed, respectively. The $u = \delta$ is the input control signal (duty cycle), the $dis = T_L$ donates the input disturbance caused by the load torque T_L and the $y = w$ is the output system speed. The linearized state matrix $A^{n\times n}$, the input matrix $B_u^{n\times 1}$ the input disturbance matrix $B_d^{n\times 1}$, and the system output matrix $C^{1\times n}$, respectively.

2.4.4 dc-dc Buck dc-Motor Discrete Time System Modeling

Modeling is conducted for the purpose of designing discrete time MPC control system. In this case study the zero-order hold (ZOH) mechanism was used to discretize the system represented in (2.38) and (2.39) over a sampling time of Ts period of time using the expression as below:

$$A_d = e^{A_{lin} * Ts},\ B_{u,d} = \int_0^{\Delta Ts} e^{A_{lin} * Ts} * B_{u,lin} * dTs, B_{d,d} = \int_0^{\Delta Ts} e^{A_{lin} * Ts} * B_{d,lin} * dTs \tag{2.40}$$

For simplicity, the MATLAB built-in c2d function is used for calculating the proposed discrete representation of the continuous system matrices [34]. Therefore, the discrete state equation takes the format as follows:

$$\begin{aligned} z(k+1) &= A_d * z(k) + B_{d,u} * u(k) + B_{d,d} * dis(k) \\ y(k) &= C_d * z(k) \end{aligned} \tag{2.41}$$

where the state *vector is the* $z(k) = [iL\ vC\ iM\ w_m]^T$ and $u(k)$ is the control input variable, $dis(k)$ is the input, disturbance, the $y(k)$ is the system output, and k is discrete time sampling period, and the discrete time system matrices are A_d is state matrix, the $B_{d,u}$ is the input matrix, the $B_{d,d}$ is the input disturbance matrix, and the C_d is the output matrix.

CHAPTER THREE

MODEL PREDICTIVE CONTROL (MPC) FOR LINEAR DISCRETE TIME SYSTEM

The principle of the MPC control system is that it has access to an accurate mathematical discrete model of the proposed plant system in order to predict the future states (x) and the future control input signal (u) over a number of prediction horizon intervals used to predict the future behavior of the plant output (y) to track the desired reference signal (r) [4] and [5].

One of the MPC controller advantages against the conventional control system such as the PID or the LQR, is that its ability to apply hard constraints [35]. As it is proposed in this dissertation, the formulation of the MPC is optimized to solve the constrained quadratic programming (QP) problem in which the optimization process can be presented on the current and future prediction intervals. In this chapter, the proposed plant models will be considering the assumptions below:

Assumption 3.1 The proposed systems are discrete time systems, formulated as Linear Time Invariant (LTI) in a state space format, the MPC formulations will be tested with a system which is not subjected to any types of parameters uncertainties or additive disturbances, then the same MPC formulation will be tested with another system which is effected with an input disturbance but the parameters values are known.

Assumption 3.2 The MPC control system is designed with a system model. which is subjected to linear constraints applied to the input control signal.

3.1 Prediction Process Design

The MPC processes are based on the minimization of the predicted performance of the objective cost, which is defined in the predicted input control signal $U(k)$ and the predicted states $Z(k)$. For that reason, the accuracy in the MPC performance is based on the accuracy in the prediction of those vectors. Therefore, calculating the perfect discrete state space model is one of the ways that it can be used to predict the states and the input vectors [4]-[6] and [35],[36].

$$\begin{aligned} z(k+1) &= A_d z(k) + B_{d,u} u(k) \\ y &= C_d z(k) \end{aligned} \tag{3.1}$$

Note that the representation in (3.1) shows that this system is single input single output and no input or output disturbance are disturbing this system, where $A_d, B_{d,u}, C_d$, and D_d are the discrete system matrices, z, u,and y are the system state, input control signal (the manipulated variable) and the system output (measured output) at k (where $k > 0$) is the discrete time period.

Considering the system represented in (3.1), the future sequences of the state vector $Z(k)$ can be predicted over a number of prediction horizon intervals Np (the Np is known as the optimization process duration), and the future input control signal $U(k)$ is counted for a duration of control horizon Nc intervals (where the $Nc \leq Np$). Both the $U(k)$ and $Z(k)$ are represented to take the form as below [4]-[6] and [34]-[36].

$$U(k) = [u(k|k)\ u(k+1|k)\ \dots\ u(k+Nc-1|k)]^T \tag{3.2}$$

$$Z(k) = [\ z(k+1|k)\ z(k+2|k)\ \dots\ z(k+Np|k)]^T \tag{3.3}$$

Therefore, the future state variable based on the size of the state space matrices ($A_d, B_{d,u}$, and C_d) can be calculated as follows:

$$
\begin{gathered}
z(k+1|k) = A_d z(k) + B_{d,u} u(k) \\
z(k+2|k) = A_d z(k+1|k) + B_{d,u} u(k+1) \\
(k+1|k) = A_d^2 z(k) + A_d B_{d,u} u(k) + B_{d,u} u(k+1) \\
\vdots \\
z(k+Np|k) = A_d^{Np} z(k) + A_d^{Np-1} B_{d,u} u(k) + A_d^{Np-2} B_{d,u} u(k+1) + \cdots \\
+ A_d^{Np-N} B_{d,u} u(k+Nc-1)
\end{gathered}
\tag{3.4}
$$

And the predicted output vector calculated as below

$$
\begin{gathered}
y(k+1|k) = C A_d z(k) + C B_{d,u} u(k) \\
y(k+2|k) = C_d A_d^2 z(k) + C_d A_d B_{d,u} u(k) + C_d B_{d,u} u(k+1) \\
y(k+3|k) = C_d A_d^3 z(k) + C_d A_d^2 B_{d,u} u(k) + C_d A_d B_{d,u} u(k) + C_d B_{d,u} u(k+2) \\
\vdots \\
y(k+Np|k) = C_d A_d^{Np} z(k) + C_d A_d^{Np-1} B_{d,u} u(k) + C_d A_d^{Np-2} B_{d,u} u(k+1) + \cdots \\
+ C_d A_d^{Np-Nc} B_{d,u} u(k+Nc-1)
\end{gathered}
$$

(3.5)

The predicted state space system re-written as follow:

$$
Z(k) = V * Z(k) + P * U(k) \tag{3.6}
$$

Where

$$
V = \begin{pmatrix} A_d \\ A_d^2 \\ \vdots \\ A_d^{Np} \end{pmatrix}
$$

$$
P = \begin{pmatrix} B_d & 0 & \cdots & 0 \\ A_d B_d & B_d & \ldots & \vdots \\ \vdots & \vdots & \ddots & 0 \\ A_d^{Np-1} B_d & A_d^{Np-2} B_d & \cdots & A^{Np-N} B_d \end{pmatrix}
\tag{3.7}
$$

In case of a Multi-Input and Multi-Output (MIMO) system, the discrete time state space representation is shown below:

$$
\begin{gathered}
z(k+1) = A_d z(k) + B_{d,u} u(k) + B_{d,d} * dis(k) \\
y = C_d z(k)
\end{gathered}
\tag{3.8}
$$

In the MIMO system case the dimensions of the state, control signal, and the output are highly important, thus the future output Y(k) vectors can be formatted as in the representations below:

$$Y(k) = [\, y(k+1|k)\; y(k+2|k) \ldots\; y(k+Np|k)]^T \tag{3.9}$$

And the predicted state and the predicted output formulated based on the size of the state space matrices (A_d, $B_{d,u}$, $B_{d,d}$, and C_d) as in equations (3.10) and (3.11), respectively

$$\begin{gathered}
z(k+1|k) = A_d z(k) + B_{d,u} u(k) + B_{d,d}\, dis(k) \\
z(k+2|k) = A_d z(k+1|k) + B_{d,u} u(k+1) + B_{d,d}\, dis(k+1) \\
= A_d^2 z(k) + A_d B_{d,u} u(k) + B_{d,u} u(k+1) \\
+ A_d B_{d,d} dis(k) + B_{d,d} dis(k+1) \\
\vdots \\
z(k+Np|k) = A_d^{Np} z(k) + A_d^{Np-1} B_{d,u} u(k) + A_d^{Np-2} B_{d,u} u(k+1) + \cdots \\
+A_d^{Np-Nc} B_{d,u} u(k+Nc-1) + A_d^{Np-1} B_{d,d} dis(k) \\
+A_d^{Np-2} B_{d,d} dis(k+1) + \cdots + A_d^{Np-N}\; B_{d,d} dis(k+Nc-1)
\end{gathered} \tag{3.10}$$

$$\begin{gathered}
y(k+1|k) = C_d A_d z(k) + C_d B_{d,u} u(k) + C_d B_{d,d}\, dis(k) \\
y(k+2|k) = C_d A_d z(k+1) + C_d B_{d,u} u(k+1) + C_d B_{d,d} dis(k+1) \\
= C_d A_d^2 z(k) + C_d A_d B_{d,u} u(k) + C_d B_{d,u} u(k+1) \\
+ C_d A_d B_{d,d} dis(k) + C_d B_{d,d} dis(k+1) \\
\vdots \\
y(k+Np|k) = C_d A_d^{Np} z(k) + C_d A_d^{Np-1} B_{d,u} u(k) + C_d A_d^{Np-2} B_{d,u} u(k+1) + \\
+C_d A_d^{Np-Nc} B_{d,u} u(k+Nc-1) + C_d A_d^{Np-1} B_{d,d} dis(k) \\
+C_d A_d^{Np-2} B_{d,d} dis(k+1) + \cdots + C_d A_d^{Np}\quad B_{d,d} dis(k+Nc-1)
\end{gathered} \tag{3.11}$$

Therefore, the predicted output can be in the prediction state space

$$Y = V * z(k) + Pu * u(k) + P_d * dis(k) \tag{3.12}$$

$$V = \begin{pmatrix} C_d A_d \\ C_d A_d^2 \\ C_d A_d^3 \\ \vdots \\ C_d A_d^{Np} \end{pmatrix}$$

$$P_u = \begin{pmatrix} C_d B_{u,d} & 0 & \cdots & 0 \\ C_d A_d B_{u,d} & C_d B_{u,d} & 0 & 0 \\ \vdots & \vdots & \ddots & \vdots \\ C_d A_d^{Np-1} B_{u,d} & C_d A_d^{Np-2} B_{u,d} & \cdots & C_d B_{u,d} \end{pmatrix} \quad (3.13)$$

$$P_d = \begin{pmatrix} C_d B_{d,d} \\ C_d B_{d,d} + C_d A_d B_{d,d} \\ \vdots \\ C_d A_d^{Np-1} B_d \end{pmatrix}$$

Note due to fluctuating in the matrices A_d, $B_{d,u}$ parameters the matrices V and P might be uncertainties as well [4]-[6] and [34]-[36].

3.2 Optimization and Cost Function Calculation

The main goal of the control design is to force the system output to track the reference signal $r(k)$ along the prediction horizon Np. The reference signal can be defined as $r(k) = [r(k+1), r(k+2), \dots, r(k+Np)]^T$. Therefore, the general cost function that is used to get the best value for the vector U that minimizes the error between the system predicted output and the reference signal is defined in (3. 14) [4]-[6] and [34]-[36].

$$\underbrace{\min}_{J(k)} = \sum_{i=0}^{Np-1} \left[\left(Z(k+i|k) - r(k+1) \right)^T \bar{Q} \left(Z(k+i|k) - r(k+1) \right) + U^T(k+i|k) \bar{R} * U(k+i|k) \right] \quad (3.14)$$

With the consideration of Q and R positive definite matrices (Q can be semi-definite). Replacing $Z(k)$ in the expression (3. 6) in case of the SISO system, and in

expression (3.12) in case of the MIMO system that will reformulate a new cost function equation as below [4]-[6] and [35]-[37]

$$J(k) = U^T(k)HU(k) + 2Z^T(k)f^TU(k) + Z^T(k)GZ(k) \quad (3.15)$$

$$\text{s.t} \qquad A_{inq} * U(k) \leq b_{inq} \quad (3.16)$$

where the A_{inq} and the b_{inq} represent the inequality constraints that are applied to the input control signal. The inequality constraints can be re-written in vector terms as below [4]-[6] and [35]-[37].

$$\begin{bmatrix} I \\ -I \end{bmatrix} \leq U(k) \leq \begin{bmatrix} 1\overline{u} \\ -1\underline{u} \end{bmatrix} \quad (3.17)$$

And

$$H = P^T\overline{Q} + R \quad (3.18)$$

$$f = P^T\overline{Q}V - r^T\overline{Q}P \quad (3.19)$$

$$G = V^T\overline{Q}V + \overline{Q} \quad (3.20)$$

With

$$\bar{Q} = \begin{bmatrix} Q & 0 & \dots & 0 \\ 0 & \ddots & & \vdots \\ \vdots & & Q & 0 \\ 0 & \cdots & 0 & Q \end{bmatrix}, \quad R = \begin{bmatrix} R & 0 & \dots & 0 \\ 0 & \ddots & & \vdots \\ \vdots & & R & 0 \\ 0 & \cdots & 0 & R \end{bmatrix} \quad (3.21)$$

In order for the objective cost function to be solved as a convex optimization problem, the hessian matrix H must be a positive definite or semi definite matrix and the constraints are linear.

Since the MATLAB is the implementation tool, the Q P problem will be solved using the (***quadprog***) function which can be defined in terms of the matrices/vectors H ,f,

and the inequal constraints A_{inq} and b_{inq}, as in the expression below [4]-[6] and [35]-[37].

$$\mathrm{U_{pred}} = \mathrm{quadprog}\left(\mathrm{H, F, A_{inq}, b_{inq}, [\quad], [\quad]}\right) \quad \mathrm{A_{inq}Z \leq b_{inq}} \tag{3.22}$$

Since solving the QP equation generates a vector of elements, therefore the receding horizon method will therefore be used to pick only the first element of the generated elements [36] and [37]

$$\mathrm{U(k)} = [1\ 0\ 0\ 0] * \mathrm{U_{pred}} \tag{3.23}$$

3.3 Case Study I The Model Predictive Control of DC-DC Buck-Boost Converter with Various Resistive Load Values

3.3.1 The Converter Modeling Process

In this case study, the theory of a constrained MPC is proposed for a dc-dc Buck-Boost converter, as it is shown in Fig. 3.1. The proposed dc-dc buck-boost converter is a single-input single-output control system as previously modeled in chapter 2. For the aim of linear and discrete time control system design, the proposed converter's mathematical

state-space model discretized using the zero-order hold (ZOH) method. The continuous state space equation (2.22) discretized over a sampling time Ts using the following expression

$$\mathrm{A_d} = \mathrm{e^{Acon*Ts}} \quad \mathrm{B_{d,u}} = \int_0^{\mathrm{Tp}} \mathrm{e^{Acon*Ts}}\ \mathrm{dTs} \tag{3.24}$$

Since the MATLAB is used for this case study, the c2d built-in function can be used to discretize the system at sampling time Ts sec to take the form of the discrete state space equation, as illustrated in (3.1).

Considering the parameters' values listed in the Table 3.1, the linear discrete time system matrices $A_d, B_{d,u}, C_d,$ and D_d numerically are illustrated as below:

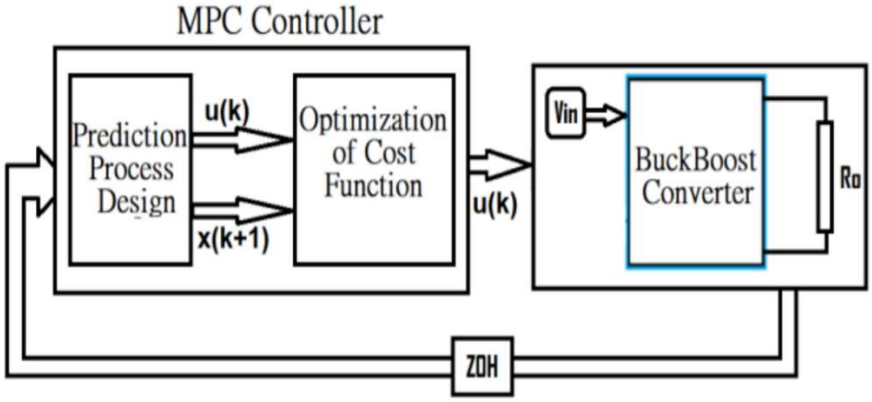

Fig. 3.1 The schematic diagram of MPC and dc-dc buck-boost converter

$$A_d = \begin{pmatrix} 0.9999 & -0.0001 \\ 0.1235 & 0.9959 \end{pmatrix},$$

$$B_{d,u} = \begin{pmatrix} 0.0400 \\ 0.0025 \end{pmatrix} \tag{3.25}$$

$$C_d = (0 \quad 1), \; D_d = 0$$

By applying the controllability and observability tests the system is controllable and observable, since the buck-boost converter is a second order n=2 and the rank of the controllability matrix $\mathrm{Crb} = 2$ and observability matrix $\mathrm{Obv} = 2$.

$$\mathrm{Crb} = (B_{d,u} \quad A_d * B_{d,u}) \rightarrow \mathrm{Crb} = 2 = n, \quad \mathrm{Obv} = (C_d \quad C_d * A_d) = 2 = n \tag{3.26}$$

Table 3.1. the parameters for the converter design

Parameters	Sample	Value
Input voltage	Vin	20V
Inductor	La	200 m H
Inductor resistive	rL	100 m Ohm
Capacitor	Ca	200 u F
Resistor load	Ro	vary Ohm
Switching frequency	fs	10 kHz
Sampling time	Ts	0.0001 sec
Duty cycle	δ	Calculated

3.3.2 Single Input Single Output Control System Process

Following up with the MPC control design process as presented in the earlier subsection, the prediction design process using the linear discrete time is used to predict the future behavior of the control signal U and the system state vectors expressions (3.2) and (3.3). The compact form of the predicted state space (3.7) and the new compact form of the matrices in (3.8) are used for the prediction modeling.

The optimization QP problem (3.15) is subjected to inequality constraints in (3.16) with consideration of the positive definite Q and R matrices as they are valued in (3.27) over a prediction horizon Np=30. Considering calculation of the Hessian H as a positive definite matrix (can be positive semidefinite), the vector f and the scaler G are calculated based on the Z(k), as illustrated in (3.18) - (3.20).

$$R = 0.01, \qquad Q = \begin{pmatrix} 1000 & 0 \\ 0 & 1000 \end{pmatrix} \tag{3.27}$$

Therefore, the optimization can be calculated using the MATLAB built-in function "***quadprog***" and the constraints represented in the expression (3.22) to predict a stack of elements in each sampling of time. Since the system is a SISO system, only one input control signal is needed; thus, the receding horizon technique is applied to pick only the first element at each sampling instant, as in the expression illustrated in (3.23).

3.3.3 Simulation Results

The proposed control system for the Buck-Boost converter was implemented and simulated using the MATLAB and Simulink environments which are carried out on a laptop-computer with 16GB RAM and CORE i7 1.8 GHZ CPU and Windows 10 professional operating system.

The simulation study refers to the converter start-up with a fixed value of the input voltage Vin = 20V. The reference trajectory voltage for the output voltage is stated at 60V, 30V and 10V, testing the capability of the proposed control system to track the reference trajectories $Vref$. The control system is also examined when the resistive load Ro took different values of 15 and 30 Ohms.

Fig. 3.2 (A and B) illustrate the reaction of the proposed control system when the Ro = 15 ohm. In Fig (A), it shows the input control signal $u(k)$ generated for the Buck - Boost converter to regulate the required output volt and current. It is visible in Fig (B) that the converter output voltage is smoothly tracking the reference voltage signal at every stage.

The figure also shows that compared to the input voltage $Vin = 20V$ the converter is operating in both modes, as a boost converter at the time intervals from 0 to 0.5 sec the output voltage vo = 60V and vo = 30V with a small percentage of an overshoot 0.96% and inductor current iL = 3.976A. In Fig.3.3 (A) the required input control signal is u = 0.6667. On the other hand, at the time period between 0.5 to 0.7 sec, the converter requires an input control signal u = 0.1104 to operate as a buck converter and quickly reaches the desired output voltage vo = 10V and an inductor current of iL = 0.662A.

Fig. 3.3 (A and B) expresses the outputs of the proposed control system when the Ro = 30 Ohm. In Fig. 4 (A), it illustrates the input control signal $u(k)$ where it is constrained from 0 to 0.6619. This value is the maximum value for the converter to regulate the output volt of vo = 60V and inductor current iL = 1.98A. It also should be noted that the output voltage maximum overshoot percentage increased to 1.2% as compared to the Fig. 3.2(B). This is presented in Fig. 3.3 (B). At the time period between 0.5 to 0.7, the converter easily works to step-down the output voltage to reach the value of vo = 10V and inductor current iL = 0.33A that requires an input control signal of u = 0.1103.

A

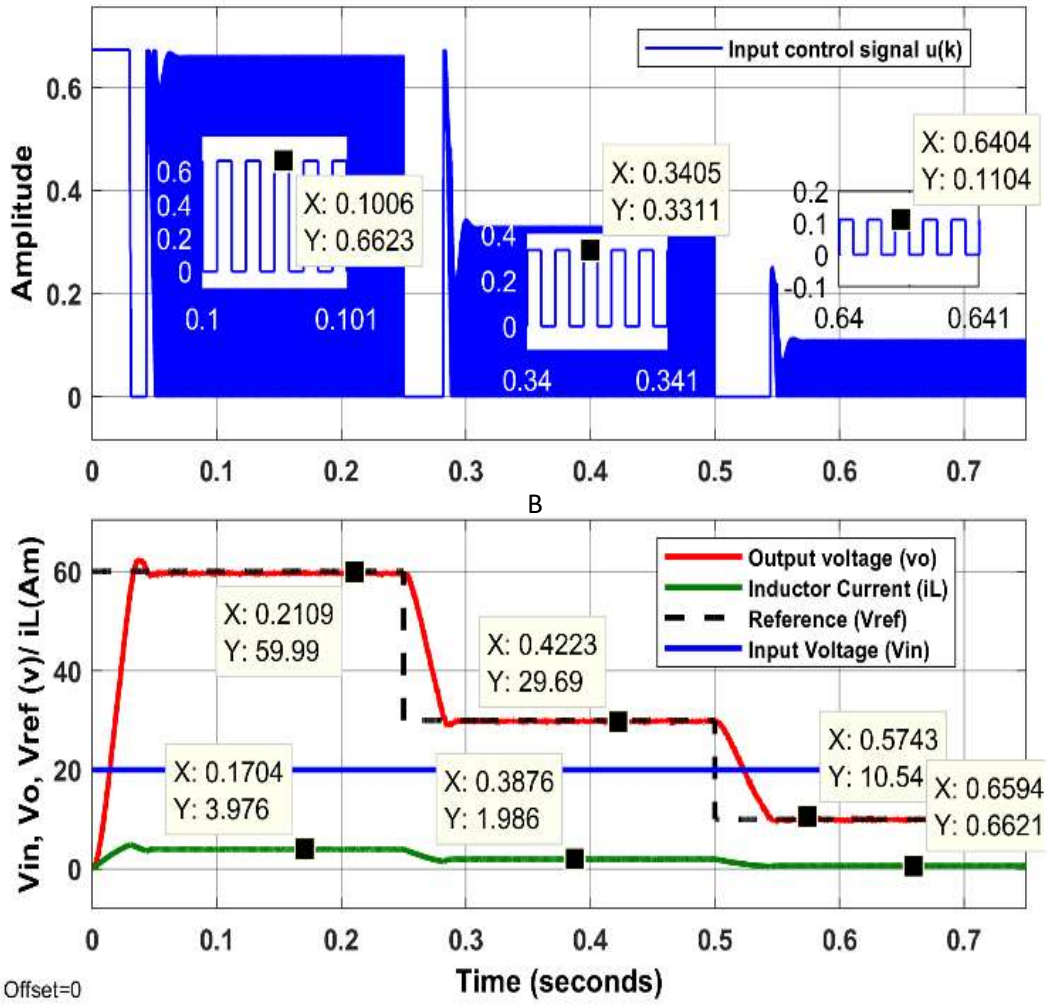

Fig.3.2 (A) show the Input Control signal (u), (B) the Output Voltage (vo) and the Inductor Current (iL)

A

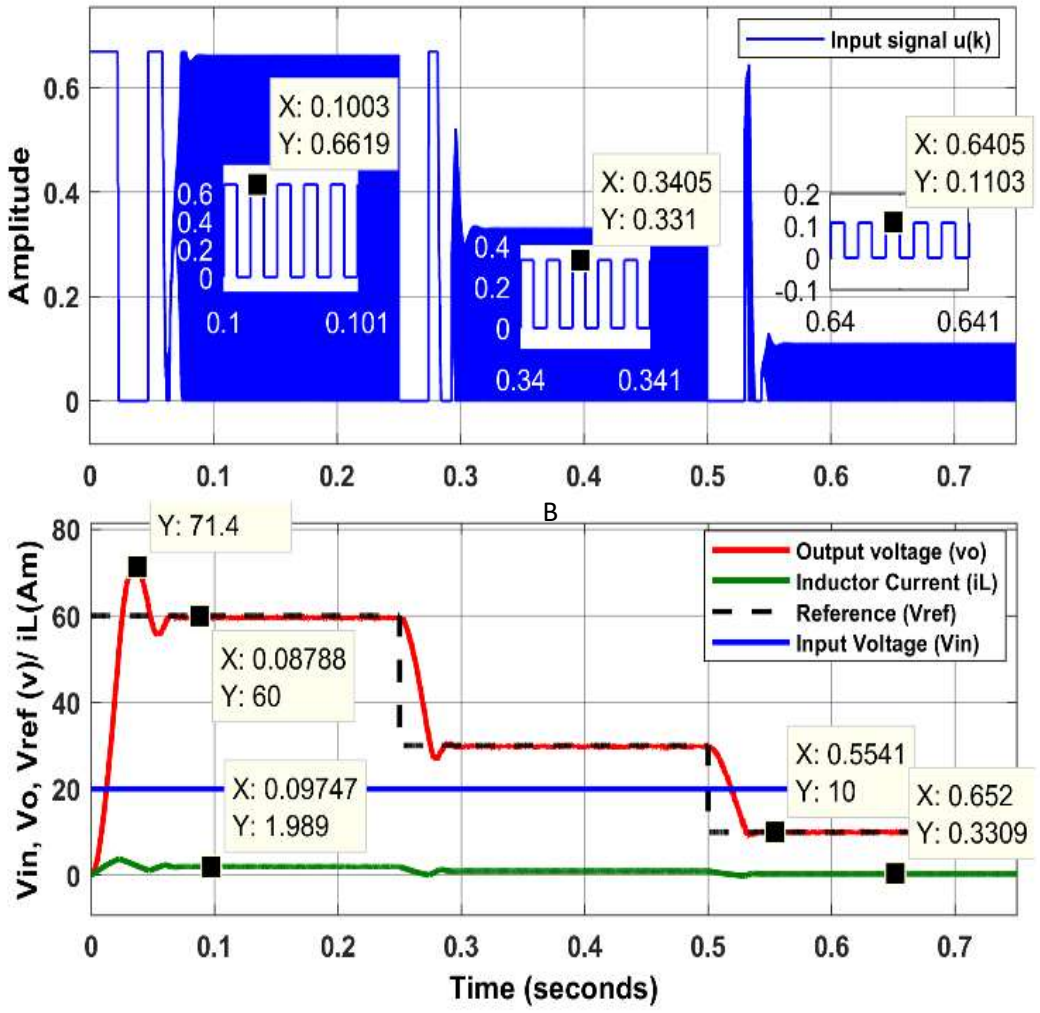

Fig.3.3 (A) show the Input Control signal (u), (B) the Output Voltage (vo) and the Inductor Current (iL)

3.4 Case Study II . Model Predictive Speed Control of dc-dc Buck Converter Driven dc-Motor with Various Load Torque Values

3.4.1 The System Model Design

In this case study, the MPC control system was tested when the dc-dc converter connected to a different type of load such as the permanent magnet direct current (dc-

motor). The dc-dc buck converter driven dc-motor is modeled and analyzed as previously presented in the subsection (2.2). The system model is a Multi-Input Single Output (MISO) system and the MPC control algorithm is optimized using the QP problem, which is subjected to inequality constraints in (3.15) and (3.16).

3.4.2 Multi Input Single Output Control Design

In this subsection, the MPC control system process will be presented for the proposed dc-dc buck converter driven dc-motor. This system model is a fourth order system and is a MISO system. In this model, the control signal u is used as a manipulated variable (MV) and the load torque T_L is considered as an input disturbance (unmeasured disturbance UD). The system output is the angular velocity w (measured output MO), the system states are the inductor current iL, the capacitor voltage vC, the armature current iM, and the angular velocity w_m.

3.4.3 The Prediction Processes

In the case of the output prediction in a MISO system where the angular velocity w_m is measured output, the predicted state $Z(k)$ and predicted input control $U(k)$ vectors are represented in (3.2) and (3.3), respectively. The prediction modeling is calculated and represented in equations (3.13) and (3.14).

3.4.4 Optimization and Cost Function Calculation

In the optimization process, the goal is to calculate the optimal solution for the objective function which will be used as the predicted control signal for the dc-dc buck converter driven dc-motor angular velocity to track the defined reference signal $r(k) = [r(k+1), r(k+2), \dots, r(k+Np)]^T$along the prediction horizon interval. Therefore, the expressions (3.15)-(3.16) are used to design the general QP cost function.

Since this case study aims to control the angular velocity, the converter is used to regulate the required voltage and current which is fed to the dc-motor. Therefore, generating the proper input control signal will directly influence the converter to regulate the desired amount of the voltage and current for the dc-motor. To this end, applying the constraints to the control signal $u \in [0,1]$ (the converter duty cycle) will dictate the converter to provide the right output power necessary for the dc-motor to track the reference signal. The linear constraint formulas (3.34) and (3.35) applied to the input control signal are shown below, both of which are subjected to the proposed cost function (3.15).

$$\underline{u} \leq u(k) \leq \overline{u} \tag{3.28}$$

Which can be formulated as

$$M = \begin{pmatrix} -I \\ I \end{pmatrix}_{2\times Nc} U(k) \leq \begin{pmatrix} 0\underline{u} \\ 1\overline{u} \end{pmatrix}_{1\times Np} \tag{3.29}$$

The 1s are indicating a stacked format of ones, and the 0s are indicating a stacked format of zeros. The expression (3.35) will be reformulated as inequal constraints to take the form of equation (3.36)

$$M * U(k) \leq \lambda \tag{3.30}$$

The M and λ are unequal constraint matrices that can be calculated offline. The optimization process of the quadratic cost function (3.28) and the subjected constraints (3.35) can be solved in MATLAB using the "***quadprog***" function as in (3.22).

Due to the process of the *'**quadprog**'* function, which generates a stack of elements, the receding horizon principle is used to pick the only first elements of the U_{pred} as in the expression below:

$$U(k) = [1\ 0\ 0\ 0] * U_{pred} \tag{3.31}$$

3.4.5 Disturbance Estimator

In the case of such a system with an input disturbance, the system states might become unmeasurable. Therefore, in this case, the MPC control system uses the static Kalman filter as a state observer [38].

In this case study, the dc-motor load torque is constant load. To get an offset free tracking of the system output (angular velocity w), an external estimation loop (Kalman filter (KF)) is added to provide the states estimations as well as help to address the load torque invariant status. The first step is to get the Kalman gain to consider the system in equation (2.40), which includes the disturbance covariance $dis(k)$.

The $dis(k)$ is represented as a white Gaussian noise with normal probability distribution. Since the measured output is the angular velocity/speed w of the system dc-dc buck converter driven dc-motor, the estimated state $\hat{z}(k)$ is possible to be calculated using the measured system output w where the $\hat{y}(k) = w_m(k)$.

$$\begin{cases} \hat{z}(k|k) = \hat{z}(k|k-1) + K_g\big(y(k) - \hat{y}(k)\big) \\ \hat{z}(k+1|k) = A_d\hat{z}(k|k) + B_{d,u}u(k) \\ \hat{y}(k) = C_d\hat{z}(k|k-1) \end{cases} \tag{3.32}$$

And the Kalman gain matrix K and the Algebraic Riccati equation parameter P for estimating the error are calculated as below

$$\begin{cases} K_g = PC_d^T R \\ A_d P A_d^T - A_d P A_d^T\big(C_d P C_d^T + R\big)^{-1} C_d P A_d^T + Q = 0 \end{cases} \tag{3.33}$$

Where the Q and R are considered as the designer parameters, the $\hat{z}$ and $\hat{y}$ are the estimated system states and output, the u is the control system signal, and the A_d, $B_{d,u}$ and C_d are the system discrete time matrices.

Therefore, the estimated system in (3.32) is used with the MPC control system prediction model every time it is inside the given prediction horizon window [38].

Using the MATLAB function, the Kalman gain K_g calculated as illustrated in the matrix $K_g = [0.12 \quad 0.24 \quad 0.13 \quad 0.88 \quad 0.0]^T$

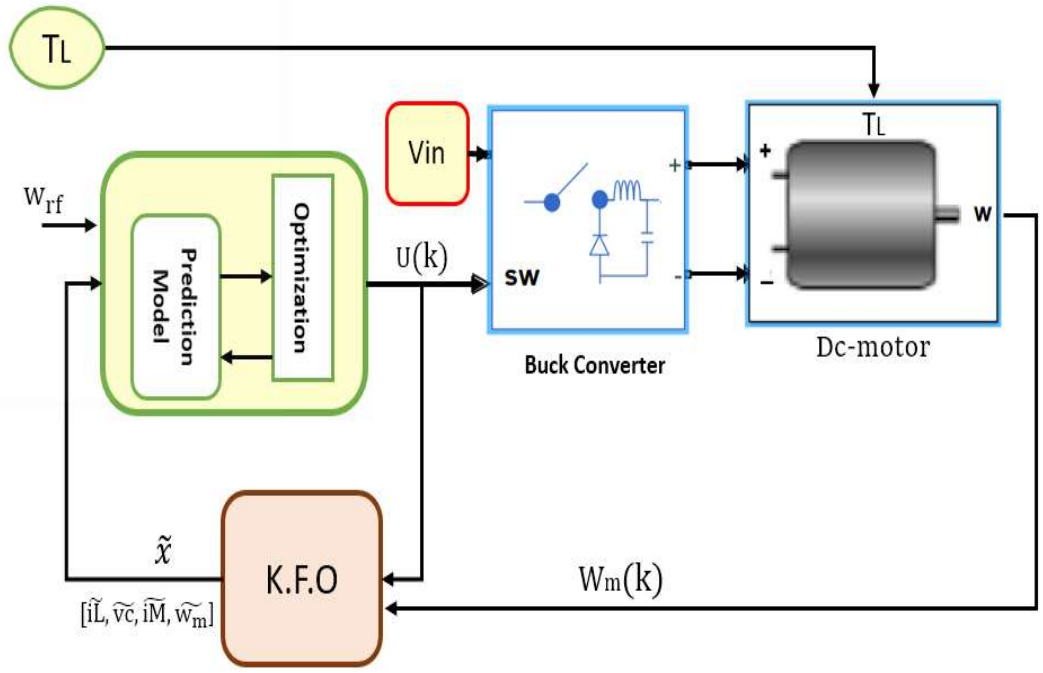

Fig. 3.4. The schematic diagram of dc-dc buck converter driving dc-motor with MPC controller

3.4.6 Simulation Output and Results

For the numerical simulation and results, the parameters' values for the proposed dc-dc buck converter-driven dc-motor are described in the Table 3.2, in which the linear discrete-time state-space system (2.40) was used to calculate the prediction modeling.

Solving the quadratic programming optimization problem has been completed through the equation (3.23) considering the prediction horizon $\mathrm{Np} = 10$ and 100.

The matrices R and Q were chosen as in equation (3.35), and the input control constraint formulated as in (3.29) and (3.30). The receding horizon equation (3.32) was used to consider the first element in every sampling instant over the prediction horizon.

$$\mathrm{R} = 1, \quad \mathrm{Q} = \begin{pmatrix} 10\mathrm{e}6 & \cdots & 0 \\ \vdots & \ddots & \vdots \\ 0 & \cdots & 10\mathrm{e}6 \end{pmatrix}_{\mathrm{Np}\times\mathrm{Np}} \tag{3.35}$$

The configuration of the proposed control system in Fig.3.4. implemented and functioned using the MATLAB and SIMULINK (version R2021B) which are carried out on a laptop computer with CORE i7 1.8GHz CPU, RAM of 16 GB, and a Windows 10 professional operating system. The dc-motor is required to track the assigned reference signal at various stages with different values of the load torque.

Figures 3.5 and 3.6 show the proposed control system is highly capable of forcing the system output $\mathrm{w_m}$ to track the reference signal $\mathrm{w_m^*}$ at different values and various shapes. Fig (3.5) and (3.6) show that the control signals are constrained in between [0, 1] and Fig Bs show the system outputs are smoothly tracking the reference signal $\mathrm{w_m^*}$ with a very fast response and very small amount of steady state errors. As proposed, to test the performance of the control system when the input disturbance is added as noted below, the case of the prediction horizon is changed from $\mathrm{Np} = 10$ and 100.

$$T_L = \begin{cases} 0 \quad \text{N.m (nominal)}, & \text{time between } 0 \text{ to } 1s \\ 0.2 \ \text{N.m (load on)}, & \text{time between } 1 \text{ to } 2s \\ 0 \quad \text{N.m (nload off)}, & \text{time between } 2 \text{ to } 3s \end{cases} \tag{3.36}$$

Table. 3.2 the dc-dc buck converter and the dc-motor parameter values

Parameter	Sample	Values
Input Voltage	Vn	40v
Converter Inductor	L	2.473 mH
Converter Capacitor	C	46 uF
Switching frequency	F	10 kHz
Duty cycle	δ	0.6
Inductor internal resistor	rL	0.695 ohms
Armature resistor	Rm	2.7 ohm
Armature inductor	Lm	1.7 mH
Viscosity fraction coefficient	B	0.000138 N.m/rad/sec
Inertia moment	Jo	0.000115 Kg.m^2
Motor torque constant	Km	0.0663 N.m/A
Voltage constant	ke	0.0663 V/rad/sec
Load torque	T_L	Vary N.m

Fig. 3.7 A, B, C illustrate the input control signal, the system angular velocity/speed, the converter voltage, current, and the dc-motor armature current when the prediction horizon Np =10 and the load torque are proposed in (3.36). As illustrated in Fig. 3.7 A, the input control signal is constrained between [0 1]. In Fig 3.7 B, although the load torque is varied from 0 to 0.2 N. m to 0 again, the control system performs very well to keep the system output w tracking the w^*, although there was a small percentage overshooting of 0.125% when the T_L raised up to 0.2 N. m and 0.05% when the T_L took it off to 0 N. m. In terms of the power supply, the dc-dc buck converter successfully made the dc-motor smoothly start with less power consumption and the converter output voltage VC always remained less than the converter input voltage Vn. The inductor current iL and the armature current iM both have the same values; they raise up as the load torque increases, as shown in Fig. 3.7 C.

In Fig. 3.8 A, B, C the prediction horizon is Np = 100 and the control horizon is Nc =3. In Fig. 3.8 B, the performance was slightly enhanced where there is no steady state error, but despite overshoot percentage 0.35 when $T_L = 0.2$ N. m at 1 sec and -0.4 when the $T_L = 0$ at 2 sec, the output signal gets to the steady state in about 2×10^{-3} sec. The power consumption in Fig. 3.8 C remains the same with no change compared to the previous figures 3.7 when the Np =10.

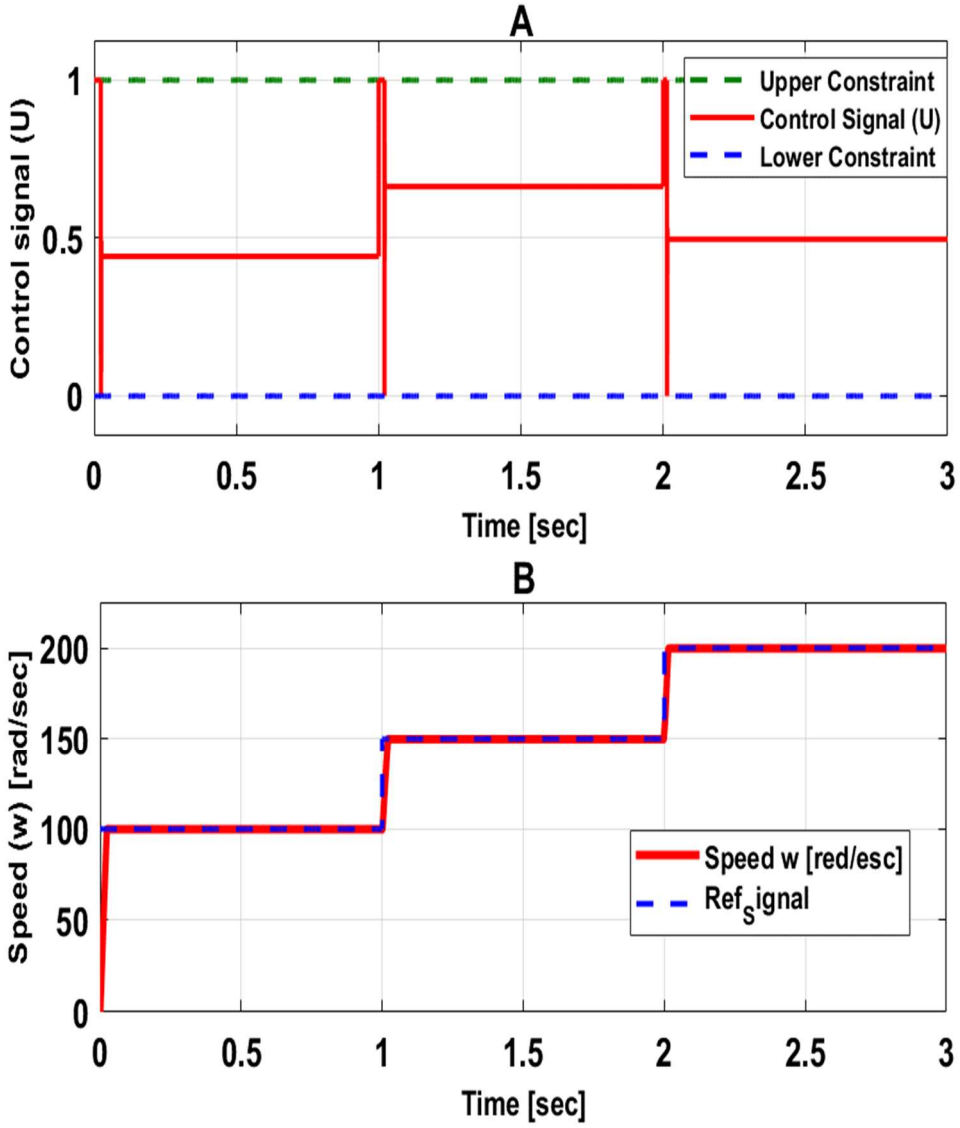

Fig.3.5 (A) the Control Signal and (B the dc-motor speed at different speed

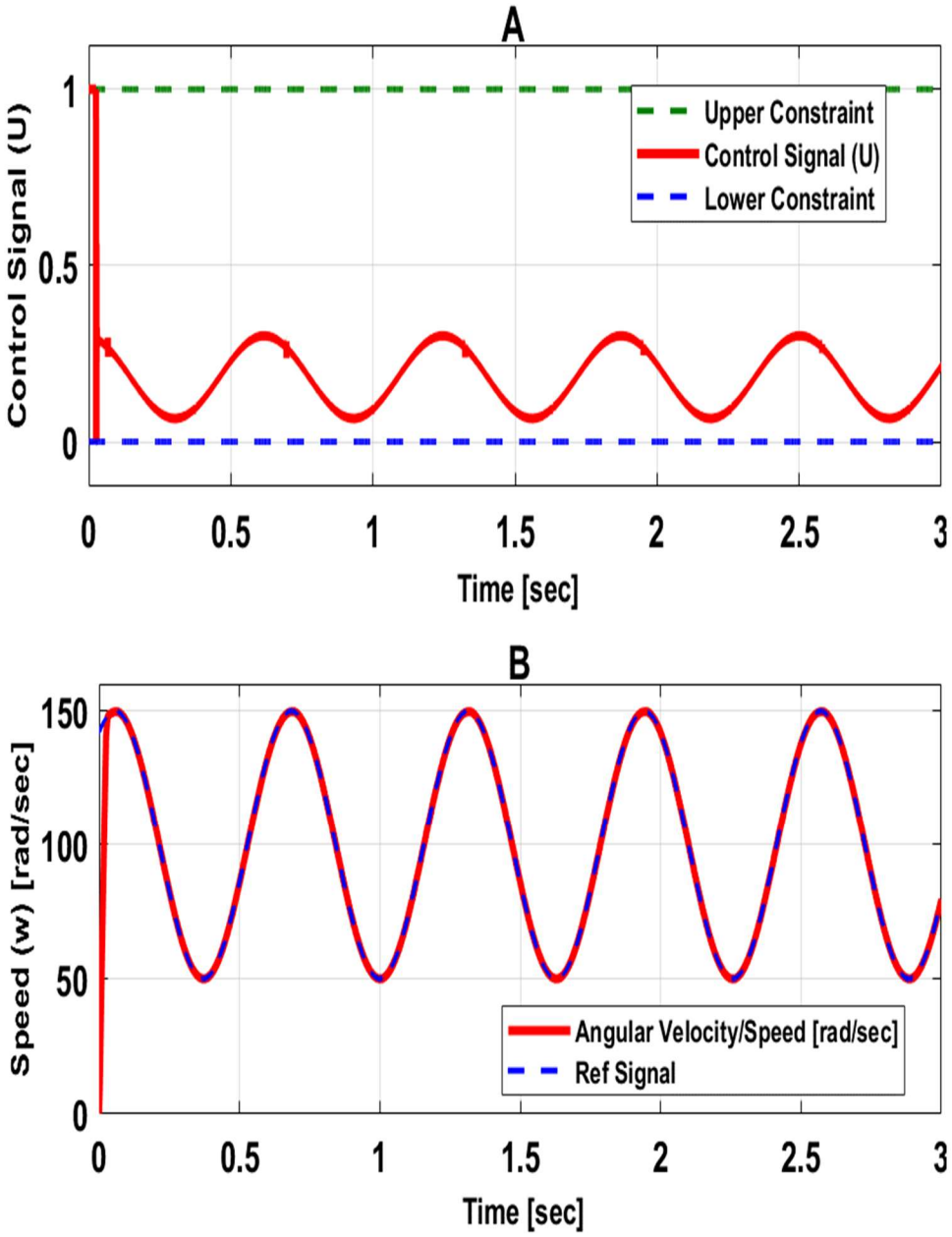

Fig. 3.6 (A) shows the system input control signal (U), and (B) the system output Angular Velocity w when the reference Angular Velocity signal w^* assigned as a sine wave signal

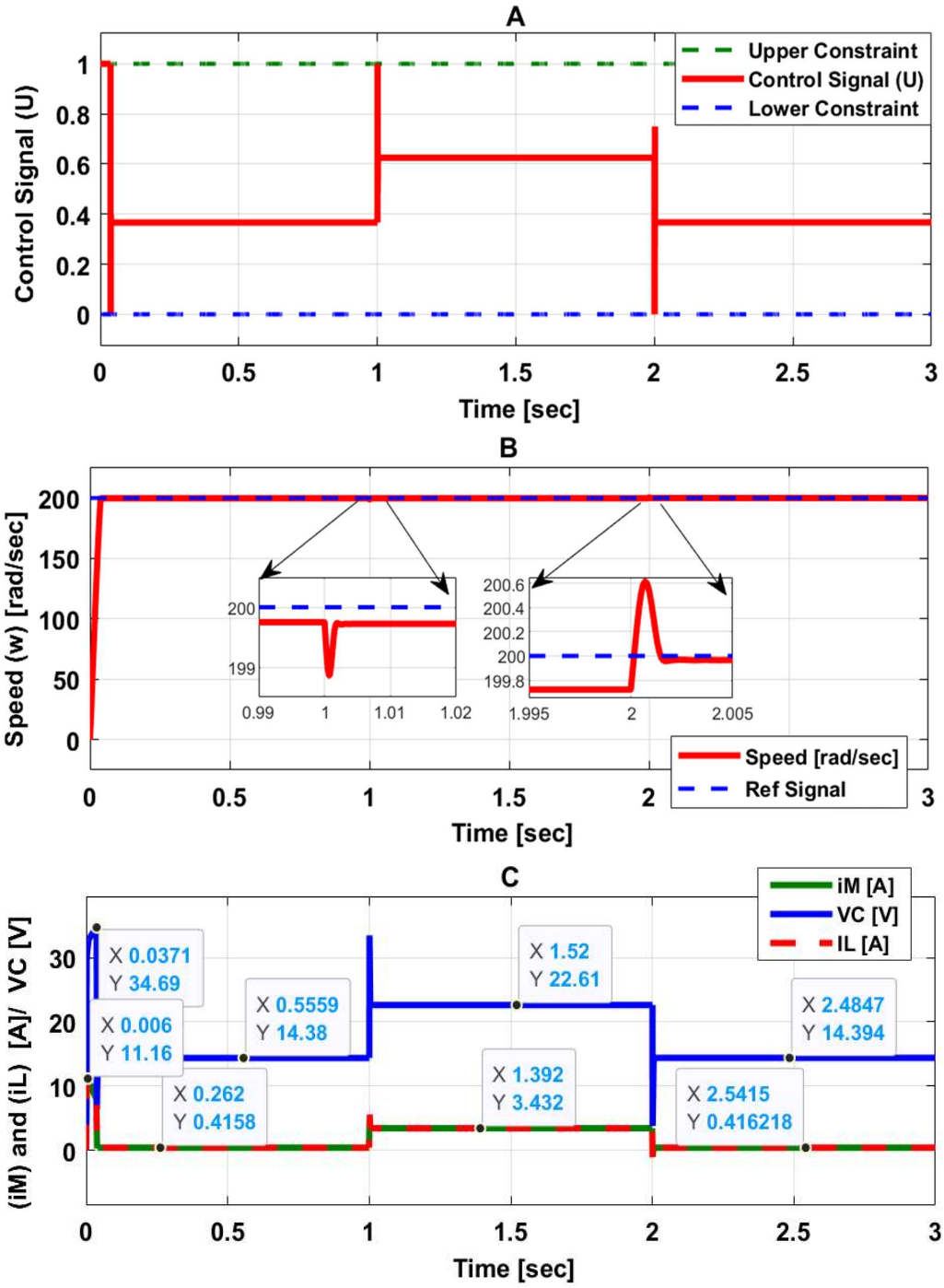

Fig. 3.7 (A) input control signal (U), (B) the system output Angular Velocity w when the reference Angular Velocity signal w^* and (C) is the converter voltage VC, the inductor current iL and the armature current iM when $Np = 10$ and $Nc = 3$.

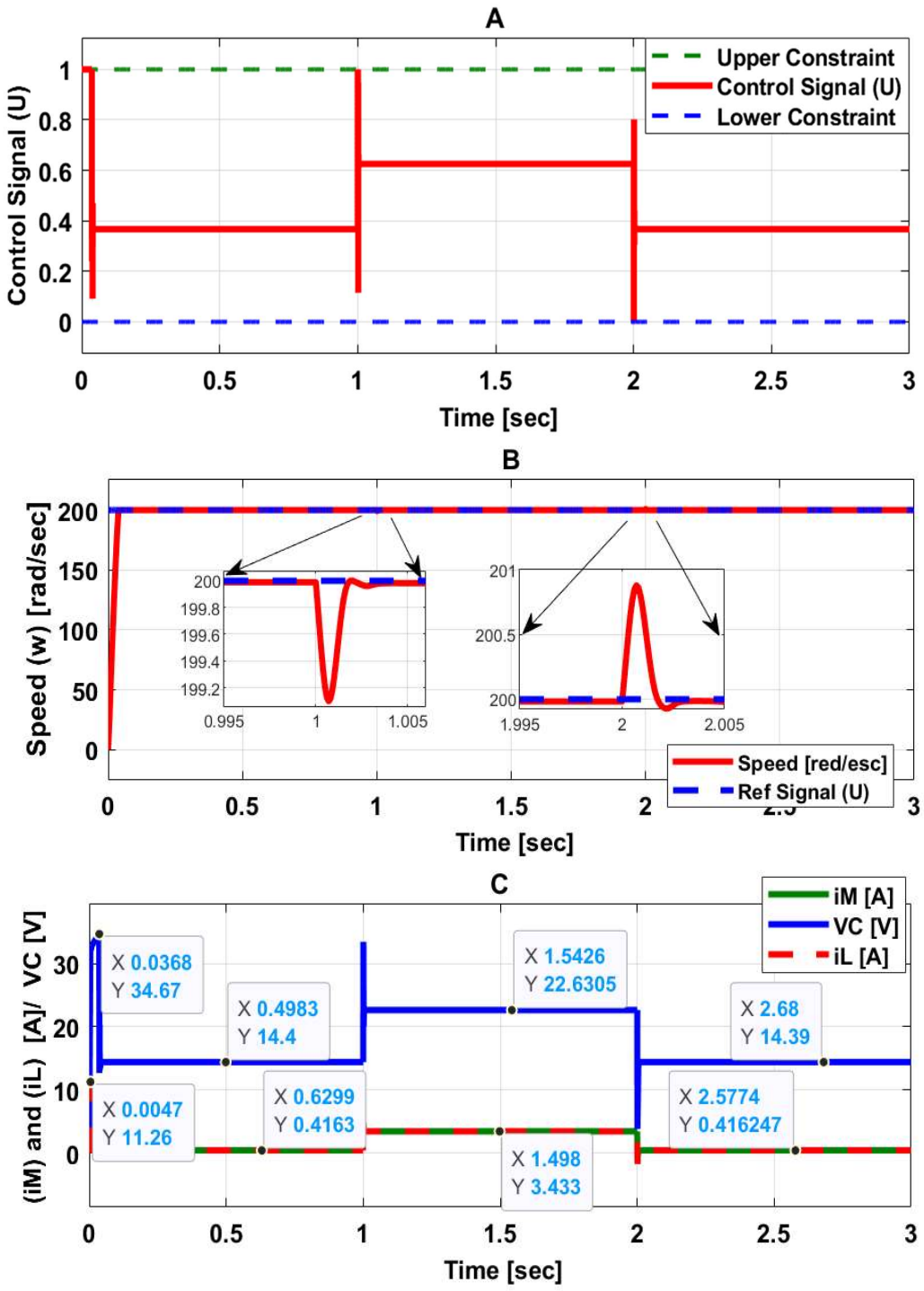

Fig. 3.8 (A) shows the system input control signal (U), and (B) the system output Angular Velocity w when the reference Angular Velocity signal w^* and (C) is the converter voltage VC, the inductor current iL and the armature current iM when Np $= 100$ and $Nc = 3$.

3.5 CHAPTER CONCLUSION

In summary, this chapter discussed the implementation of the MPC control system to enhance the work performance and to maintain a clear and constant output of the proposed power electronics and industrial applications. In both case studies, a linear MPC control strategy with inequality constraints was applied to the proposed systems, which were linear and in a discrete-time state-space format. The state-space models were used over a prediction horizon interval to generate the predicted system matrices, which will be used in the optimization process. The QP problem and the subjected inequality constraints were optimized to calculate the optimal solution for the predicted input control signal at each sampling time interval, the constraints were applied to limit the input control signal within the range of the required duty ratio. In the case study I, as was mentioned earlier; the dc-dc buck-boost converter was stable and linear, and the goal was to design the proposed controller to force the output voltage to keep tracking the reference signal at various levels in the presence of the previously mentioned problems. This change in the output level proves that the converter can be used in both the buck operation mode and the boost operation mode even with the change of values of the connected resistive load and at different prediction horizon intervals; this has been proved in the figures above. In case study II, the control system showed a high level of performance and robustness, and the results illustrated that the dc-dc buck converter driven dc-motor could be handled successfully by the MPC controller and the assisted the KF to perform a constant speed of the proposed system even with the effect of the load torque (input disturbance). The advantage of the KF was to assist the MPC controller in observing the unmeasurable states. Also, the system output signal response was fast

enough to reach the desired tracking trajectory, even with the presence of the input disturbance.

CHAPTER. FOUR

ADAPTIVE MODEL PREDICTIVE CONTROL FOR DC-DC POWER CONVERTERS WITH PARAMETERS' UNCERTAINTIES

A system with nonlinear behaviors or its characteristics changing dramatically over time can cause a high level of degradation that cannot be handled with the conventional control systems since linearizing this system at one specific operating condition is not enough to predict the future behavior of this system accurately.

The parameters' uncertainties and the switching behavior of a dc-dc buck-boost converter can make the system strongly nonlinear, and its operating condition will vary over time. For this reason, the linearization at one operating condition is not precise to cover the converter's operation range, but it needs to be linearized at multiple of the operating conditions to perform Linear Time-Invariant (LTI) models which create what is called a Linear Parameters-Varying (LPV). Due to these changes, the Adaptive MPC-LPV control approach was proposed due to its ability to update the prediction model plant and the operating conditions. With these updates, the controller remains constant over a prediction horizon at each control interval. To ensure the high robustness and quality of proposed control approach, it was implemented in a simulation environment as well as in a real-time environment using MATLAB Simulink and Arduino Mega 2560 microcontroller, Also, the proposed control algorithm was compared with various control approaches in different operating sides.

In this chapter, the AMPC-LPV control approach was implemented to control a dc-dc buck-boost converter which was:

• Linearized at different operating conditions to perform a set of LTI models; those models define a Linear Parameter-Varying (LPV) model.

• Designed assuming that the uncertainty parameters were not precisely known but they were bounded in a min-max range.

• Applied constraints to limit the amplitude of the input control signal within a boundary of 0 and highest value of the duty cycle d.

• Its performance tested at different prediction horizons.

The AMPC control system for the proposed converter was implemented in real time using Arduino Mega 2560 microcontroller and it works well to provide the desired output voltage at different levels and in fast response.

Note in this chapter:

- The reg-MPC is donating to the standard MPC (un adaptive MPC).

- The G.S.PI is donating the gain scheduling proportional integral control system.

4.1 dc-dc Buck-Boost Dynamic System Design

In this subsection, the dynamic analysis, and calculations for the proposed dc-dc buck-boost converter will be considered as previously analyzed and derived in the subsection (2.1.1) to illustrate the averaged model of the inductor current iL and output voltage vC (2.18) and (2.19). The parameters name and samples which will be used later are the VG for the input voltage, the SW represents the switching behavior of the MOSFET, L for the inductor, **dio** for the diode, C for the capacitor, rC and rL for the capacitor and inductor resistors, R for the resistive load, Ts is the sampling time, and d for the duty cycle [23], [24], and [27].

4.2 Linear Parameter Varying (LPV) Modeling

The LPV system is a function of time-varying variables (the scheduling parameters) that define the dynamics of a system model. The LPV is configured as an array of linear state space or linear time-invariant (LTI) systems whose coefficients are dependent on the change in parameters. One of the typical representations of the LPV system is that it can be defined as a grid-based LPV system depending on the scheduling parameters. At each node of the represented grid are the values of the scheduling parameters p, which describe each related LTI system and its operating condition information. The LPV uses the interpolation and extrapolation techniques to address the most accurate LTI system conflicted by the scheduling parameters. The grid based LPV is defined depending on the changes of the scheduling parameters as a regular grid model and irregular grid model [38], [41], and [42].

- The regular grid LPV is formulated when the scheduling parameters p change monotonically over time. This type of LPV model contains multiple state-space models based on the combination values of the scheduling parameters p change linearly simultaneously as in Figure 4.1.
- The irregular grid LPV is formulated if one or more of the scheduling parameters are missing or changing at different times, as presented in Figure

Due to the switching behavior and the parameters' uncertainties, the linearization process that was previously proposed in the subsection (2.3) was not precisely enough for such a system with full fluctuated parameters over time. Therefore, the linearization of the averaged model (2.18) and (2.19) was done multiple times considering the system scheduling parameters $p(t)$ values changed randomly over time to generate a set of LTI

models (family of models) to create LPV system. The scheduling parameters can be represented as a scalar quantity or a vector of different variables to define an LPV model. In this work, the parameters' values of the proposed dc-dc converter were not precisely known; they were assumed to vary within min/max boundaries. For that issue, the linearization process was conducted over a grid of operating points. Each operating space was a subset parametrized by the scheduling parameters' values at a specific time. Over time, these subsets became a family of linear time-invariant (LTI) arrays; this configured the grid-based LPV system. To this end, the proposed dc-dc buck-boost converter's scheduling parameters were bounded in the representation as in the expression below: [38], [41], and [42].

$$R \in [\overline{R}, \underline{R}], Vg \in [\overline{VG}, \underline{VG}], L \in [\overline{L}, \underline{L}] \text{ and } C \in [\overline{C}, \underline{C}] \quad (4.1)$$

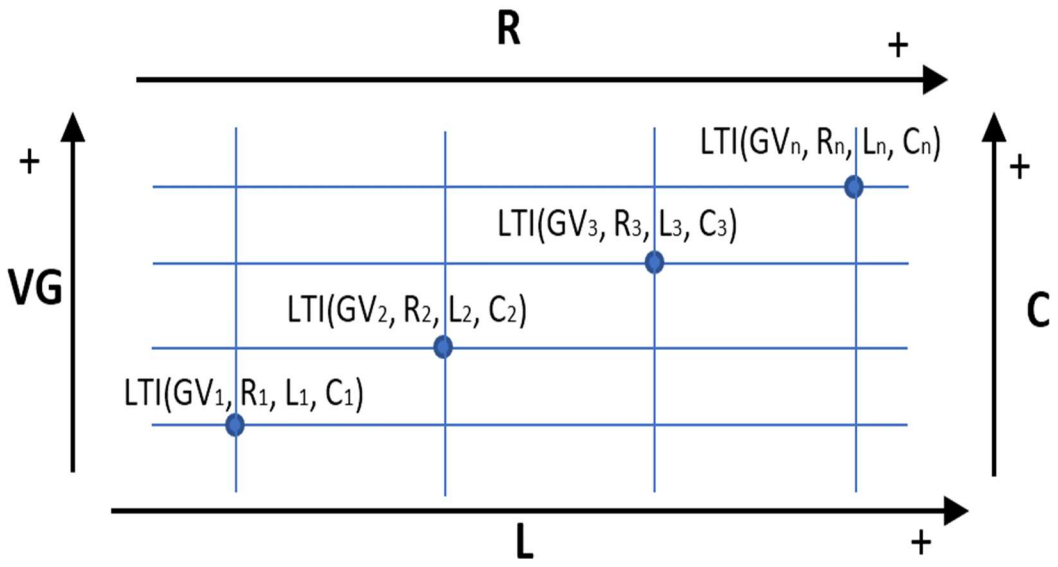

Fig. 4.1 The Regular Grid for The LPV model

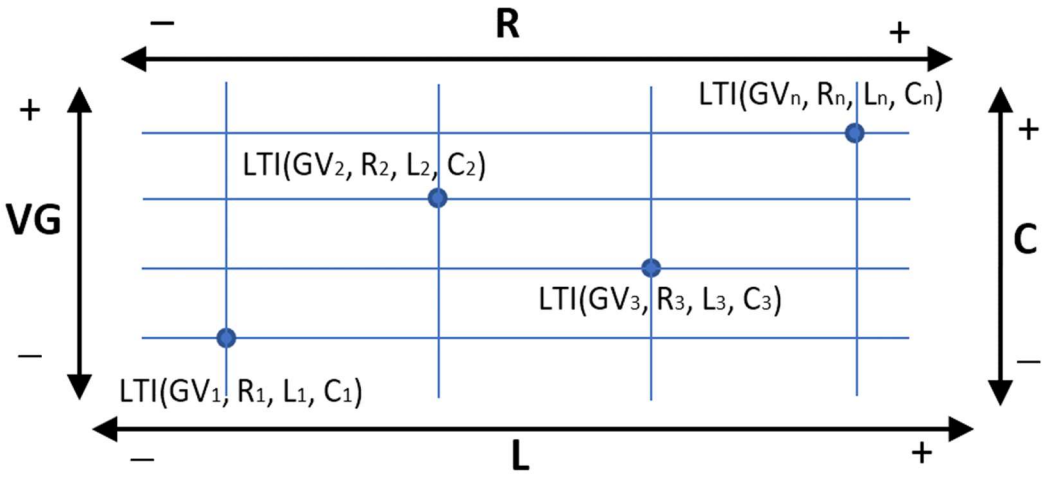

Fig. 4.2 The Irregular Grid for The LPV model

The change in the scheduling parameters' values directly affects the LPV scheduled state-space matrices $S_p = (\mathbf{A}_p(p), \mathbf{B}_p(p), \mathbf{C}_p)$, the matrix $\mathbf{C}_p$ is assumed known as in (4.3). The nominal values for the plant inputs, states, and output are specified to go with its scheduled state-space matrices parallelly. Applying the interpolation and the extrapolation method to configure the most accurate LTI model and the corresponding operating points to update the proposed AMPC control system with the changes of the system pant model. To the aim for a discrete-time control design, the set linearized LTI models are discretized using the Zero Order Hold (ZOH) method at a sampling time Ts. Therefore, the discrete LPV system can be expressed as below:

$$\begin{aligned} \tilde{x}(k+1) &= \mathbf{A_p}(p)(\tilde{x}(k)) + \mathbf{B_p}(p)(\tilde{u}(k)) \\ \tilde{y}(k) &= \mathbf{C_p}(p)(\tilde{x}(k)) \end{aligned} \tag{4.2}$$

Where k ($k > 0$) is the discrete time period, $\tilde{x}(k) \in \mathbb{R}^{2\,x\,1}$ is the system states vector, $\tilde{u}(k) \in \mathbb{R}^{1x1}$ is the control input (manipulated variable (MV)) , $\tilde{y}(k) \in \mathbb{R}^{1x1}$ is the system measured outputs (MO). The $\mathbf{A}_p(p) \in \mathbb{R}^{2\times 2}$ $\mathbf{B}_p(p) \in \mathbb{R}^{2\times 1}$ and $\mathbf{C}_p \in \mathbb{R}^{1\times 2}$ are the discrete time LPV scheduled state-space matrices depending on the scheduling parameters (p) [38], [41], and [42].

Due to the rank of the pair matrices ($\mathbf{A}_p$, and $\mathbf{B}_p$) and the matrices ($\mathbf{A}_p$, and $\mathbf{C}_p$) the system is controllable and observable.

And the LPV scheduling matrices are represented:

$$\mathbf{A_p} = \begin{pmatrix} -\frac{(-r\ )(R+rC)-(R*rC))D'}{L(R+rC)} & -\frac{RD'}{L(R+rC)} \\ \frac{RD'}{C(R+rC)} & \frac{-1}{C(R+rC)} \end{pmatrix}$$
$$\mathbf{B}_p = \begin{pmatrix} \frac{VG}{L} \\ 0 \end{pmatrix} \tag{4.3}$$
$$\mathbf{C}_p = (0 \quad 1)$$

4.3 Control System Design

As previously mentioned, the LPV model is comprised of LTI models that are linearized at various operating conditions, which can approximately describe the proposed converter working range. Therefore, the AMPC control system is the proposed control method to resolve these changes in the proposed plant model. To this end, the AMPC controller designed offline at the initial operating conditions using the system matrices $(\mathbf{A}_p(0), \mathbf{B}_p(0), \mathbf{C}_p)$ which are considered fully known. Then, the implemented AMPC at the initials will be incremented at the run time based on the information from the LPV model and the converter feedback signals [23],[27], [38], [41], and [42].

4.3.1 Adaptive Model Predictive Control (AMPC) Design

Due to the characteristics of the system parameters, the system matrices keep changing over time. The AMPC is the perfect control approach due to its capability to update the prediction model and the operating conditions every sampling time. Once they are updated, they remain constant over a prediction horizon interval. The AMPC is an online optimization based using the QP optimization approach. This optimization is tuned based on the system measurements in real-time, and the scheduling parameters predictions.

Since the cost function is a quadratic and the constraints are affine. The performing of the incremented optimization formula solved every time instant, formulated as below:

$$\underbrace{\min}_{\Delta u} \quad \sum_{m=1}^{Np-1}(\tilde{y}(k+m|k)-y_{rf}(k+m))^{T}Q_{x}(\tilde{y}(k+m|k)-y_{rf}(k+m)+\sum_{m=0}^{Nc-1}\Delta\tilde{u}(k+m)^{T}R_{u}\Delta\tilde{u}(k+m) \tag{4.4a}$$

$$\begin{gathered}\tilde{x}(k+m+1|k)=\mathbf{A_p}(p)(\tilde{x}(k+m|k))+\mathbf{B_p}(p)(\tilde{u}(k+m|k))\\ \tilde{y}(k+m+1|k)=\mathbf{C_p}(p)(\tilde{x}(k+m+1|k))\\ \tilde{x}(k|k)=\tilde{x}(k)\\ y_{rf}(k+Nr+\ )=y_{rf}(k+Nr+s-1)\\ m=[0,\ldots,Np-1]\\ s=[0,\ldots,Np-Nr\ \ ]\end{gathered} \tag{4.4b}$$

Where Np, Nc, and Nr are so-called the prediction horizon, the control horizon and the span of reference window, Q_x and R_u are the tracking error, and control input rate of change weighting matrices respectively.

At the prediction time period m, The reference state vector $\tilde{x}(k+m|k)$ is an incremental of the state vector $\tilde{x}$ at time $k+m$, depending on pre-known information at

time instant k. The input control sequence $\Delta\tilde{u}(k+m|k)$ is an incremented vector of the previous input control sequence $\tilde{u}(k-1)$, and the output reference vector $y_{rf}(k+m)$, can be predicted in advance at time period m. Therefore, cost minimization of the problem (4.4) can be done using the quadratic programming (QP) which is redefined interims of the scheduled state-space matrices S_p as below:

$$\begin{aligned} \underbrace{\min}_{\xi} \quad & \frac{1}{2}\xi^T \boldsymbol{\mathcal{H}}(p)\,\xi + \Gamma(k)^T\,\boldsymbol{\mathcal{W}}(p)^T\,\xi \\ \text{s.t.} \quad & G_{\emptyset}(k)\,\xi \le W_{\emptyset}(k)\,\Gamma(k) + \mathcal{S}_{\emptyset}(k) \end{aligned} \tag{4.5}$$

Where the $\xi \in \mathbb{R}^{n_s}$ is the optimization vector. The $\Gamma(k) = [\tilde{x}(k) \quad y_{rf}(k) \quad \tilde{u}(k-1)]$ is a vector of the variable parameters that change over time, and the matrices for the QP problem (4.5) are illustrated as below:

$$\boldsymbol{\mathcal{H}}(k) = \mathcal{M}\big(p(k)\big)^T Q_x\,\mathcal{M}(p(k)) + R_u \tag{4.6a}$$

$$\boldsymbol{\mathcal{W}}(k) = \mathcal{M}\big(p(k)\big)^T Q_x\,\tilde{\mathcal{F}}(p(k)) \tag{4.6b}$$

Where the hessian matrix $\boldsymbol{\mathcal{H}}$ and the column vector $\boldsymbol{\mathcal{W}}$ are sequences of the optimal control inputs [43]-[46].

$$W_{\emptyset}(k) = \begin{pmatrix} \bar{I} & 0 & 0 & 0 \\ \bar{I} & 0 & 0 & 0 \\ \bar{I} & \mathcal{F}(k) & 0 & 0 \\ \bar{I} & -\mathcal{F}(k) & 0 & 0 \end{pmatrix}, \mathcal{S}_{\emptyset}(k) = \begin{pmatrix} -U^{min}(k) \\ U^{max}(k) \\ -Y^{min}(k) \\ Y^{max}(k) \end{pmatrix}$$

$$\widetilde{\mathcal{F}_p}(k) = \mathcal{F}_p(k) \begin{pmatrix} I^{(n_y \times 1)} & 0 & \dots & 0 \\ \dots & \dots & \dots & \dots \\ 0 & \dots & 0 & I^{(n_y \times 1)} \\ 0 & \dots & 0 & I^{(n_y(Np-Nr)\times 1)} \end{pmatrix}, G_{\emptyset}(k) = \begin{pmatrix} -\gamma(k) \\ \gamma(k) \\ -\mathcal{M}_p(k) \\ \mathcal{M}_p(k) \end{pmatrix} \tag{4.7}$$

$$\mathcal{F}_{\mathrm{p}}(\mathrm{k})=\begin{pmatrix}\widetilde{\mathbf{C}_{\mathrm{p}}}(\mathrm{k})\widetilde{\mathbf{A}_{\mathrm{p}}}(\mathrm{k})\\ \widetilde{\mathbf{C}_{\mathrm{p}}}(\mathrm{k})\widetilde{\mathbf{A}}_{\mathrm{p}}^{2}(\mathrm{k})\\ \vdots\\ \widetilde{\mathbf{C}_{\mathrm{p}}}(\mathrm{k})\widetilde{\mathbf{A}}_{\mathrm{p}}^{\mathrm{Np}}(\mathrm{k})\end{pmatrix},\gamma(\mathrm{k})=\begin{pmatrix}\bar{\mathrm{I}} & 0 & 0 & \dots & 0\\ \bar{\mathrm{I}} & \bar{\mathrm{I}} & 0 & \dots & 0\\ \dots & \dots & \dots & \dots & 0\\ \bar{\mathrm{I}} & \bar{\mathrm{I}} & \bar{\mathrm{I}} & \dots & \bar{\mathrm{I}}\end{pmatrix}$$

$$\mathcal{M}_{\mathrm{p}}(\mathrm{k})=\begin{pmatrix}\widetilde{\mathbf{C}_{\mathrm{p}}(\mathrm{k})}\widetilde{\mathbf{B}_{\mathrm{pu}}(\mathrm{k})} & 0 & \dots & 0\\ \widetilde{\mathbf{C}_{\mathrm{p}}}(\mathrm{k})\widetilde{\mathbf{A}_{\mathrm{p}}(\mathrm{k})}\widetilde{\mathbf{B}_{\mathrm{pu}}(\mathrm{k})} & \widetilde{\mathbf{C}_{\mathrm{p}}}(\mathrm{k})\widetilde{\mathbf{B}_{\mathrm{pu}}}(\mathrm{k}) & \dots & 0\\ \vdots & \vdots & \ddots & \vdots\\ \widetilde{\mathbf{C}_{\mathrm{p}}}(\mathrm{k})\widetilde{\mathbf{A}}_{\mathrm{p}}^{\mathrm{Np}-1}(\mathrm{k})\widetilde{\mathbf{B}_{\mathrm{pu}}}(\mathrm{k}) & \widetilde{\mathbf{C}_{\mathrm{p}}}\widetilde{\mathbf{A}}_{\mathrm{p}}^{\mathrm{Np}-2}(\mathrm{k})\widetilde{\mathbf{B}_{\mathrm{pu}}}(\mathrm{k}) & \dots & \widetilde{\mathbf{C}_{\mathrm{p}}}(\mathrm{k})\widetilde{\mathbf{B}_{\mathrm{pu}}}(\mathrm{k})\end{pmatrix}$$

(4.8)

Where is the $\bar{\mathrm{I}}\in\mathbb{R}^{\mathrm{n_u}\times n_u}$, and the input and output constraints are illustrated as below

$$\begin{aligned}\mathrm{U}^{\min}(\mathrm{k})&=\begin{pmatrix}\mathrm{u}^{\min}(\mathrm{k})\\ \vdots\\ \mathrm{u}^{\min}(\mathrm{k}+\mathrm{Nc}-1)\end{pmatrix},\ \mathrm{U}^{\max}(\mathrm{k})=\begin{pmatrix}\mathrm{u}^{\max}(\mathrm{k})\\ \vdots\\ \mathrm{u}^{\max}(\mathrm{k}+\mathrm{Nc}-1)\end{pmatrix}\\ \mathrm{Y}^{\mathrm{man}}(\mathrm{k})&=\begin{pmatrix}\mathrm{y}^{\min}(\mathrm{k})\\ \vdots\\ \mathrm{y}^{\min}(\mathrm{k}+\mathrm{Np}-1)\end{pmatrix},\ \mathrm{Y}^{\max}(\mathrm{k})=\begin{pmatrix}\mathrm{y}^{\max}(\mathrm{k})\\ \vdots\\ \mathrm{y}^{\max}(\mathrm{k}+\mathrm{Np}-1)\end{pmatrix}\end{aligned}$$

(4.9)

And

$$\begin{aligned}\mathrm{Q_x}&=\mathrm{diag}\big(\mathrm{Q_x}(\mathrm{k}),\dots,\mathrm{Q_x}(\mathrm{Np}-1)\big)\\ \mathrm{R_u}&=\mathrm{diag}\big(\mathrm{R_u}(\mathrm{k}),\dots,\mathrm{R_u}(\mathrm{Nc}-1)\big)\end{aligned}$$

(4.10)

The prediction for the future refence of the scheduling parameters is computed by considering the pre-known information about the optimization vector, which is solved at $\mathrm{k}-1$ iteration over a prediction horizon Np. Thus, the AMPC process solves the optimization problem using the predicted scheduling parameters reference which keeps the objective QP cost function and the subjected constraints updated every time instant k. Since the LPV was stated with the scheduling parameters directly affecting the system dynamics and the input control signal manipulated by the AMPC process, the

approximate relationship between the LPV scheduled state-space matrices and the control signals can be defined in a linear state equation (4.11).

Therefore, iterating the discrete time LPV scheduled state space matrices $S_p = (\mathbf{A}_p, \mathbf{B}_p, \mathbf{C}_p)$ used to predict the scheduling parameters reference, and keep the AMPC parameters updated every time instant k over a prediction horizon Np [43]-[46].

$$\Delta\widetilde{X}_p(k|k) = \mathcal{F}_p\widetilde{X_p}(k) + \mathcal{M}_p\Delta U(k) \tag{4.11}$$

Where the predicted future state vector $\Delta\widetilde{X}_p(k)$, the future input control sequence $\Delta U(k)$ are the LTI vector based on the scheduling parameters S_p are incremented at each time instant k over a prediction horizon Np as below

$$\Delta\widetilde{X}_p(k) = \left[\Delta\widetilde{X}_p(k+1), \dots, \Delta\widetilde{X}_p(k+Np|k)\right]^T \tag{4.12a}$$

$$\Delta U(k) = [\Delta u(k|k), \dots, \Delta u(k+Nc-1|k)]^T \tag{4.12b}$$

And the matrices $\mathcal{M}_p$ and $\mathcal{F}_p$ are computed in (4.8) which are defined by the scheduling parameters state matrices S_p.

By incrementing the expression (4.11), the prediction of the scheduling parameters is estimated to keep the AMPC optimization of the proposed objective cost function, and the constraints (4.5) updated each time instant k over the considered prediction horizon Np.

To get the QP problem's (4.5) solved instantly over a prediction horizon interval, the scheduling parameters reference need to be defined, and the LPV scheduled state-space matrices calculated as below [43]-[46], [51], and [52].

$$S_p(k+i) = \begin{cases} S_p(k|k) & \text{if } i = 0 \\ S_p(k+i|k) & \text{if } 0 < i \leq Np \\ S_p(k+Np|k) & \text{Otherwise} \end{cases} \tag{4.13}$$

The AMPC algorithm constructed as below [43] and [46]:

Pre-known the input control sequence $U(k|k-1)$, the plant state vector $\widetilde{x_p}(k)$, the predicted state vector $\widetilde{X_p}(k)$, the plant output $\tilde{y}(k)$, the implemented set of the LPV model, the prediction matrices $\mathcal{M}_p, \mathcal{F}_p$

1) $U(k|k-1) \rightarrow u(k-1)$; *control signal*

2) $\left(x_p(k),\ y_{rf}(k),\ u(k-1)\right) \rightarrow \Gamma(k)$; *variable parameters vector*

3) $\widetilde{X_p}(k|k-1) = \mathcal{F}_p(k)\widetilde{X_p}(k) + \mathcal{M}_p(k)\Delta U(k|k-1)$;

state space vector trajectory

4) **for** $m = m: Np-1$

5) **if** $m = 0$ then $S_p(k) = S_p(p(k))$;

6) Elseif $m \leq Np-1$ then $S_p(k) = (p(k+m|k-1)$;

7) Else $S_p(k) = S_p(p(k+Np-1|k-1)$;

Looping for LPV scheduling state space information

8) **End if**; **End if**; **End for**;

9) $\boldsymbol{\mathcal{H}}(\mathbf{k}) = \mathcal{M}(k)^T Q_x(k)\mathcal{M}(k) + R_u(k)$

10) $\boldsymbol{\mathcal{W}}(\mathbf{k}) = \mathcal{M}(k)^{\mathbf{T}}\mathbf{Q_x}(k)\mathcal{F}(k)$

11) $G_\emptyset(k) = G_\emptyset\left(S_p(p(k)), \dots, S_p(p(k+Np))\right)$

12) $W_\emptyset(k) = W_\emptyset\left(S_p(p(k)), \dots, S_p(p(k+Np))\right)$

13) $z^*: \underbrace{\min}_{\xi} \quad \frac{1}{2}\xi^T \boldsymbol{\mathcal{H}}(p)\,\xi + \Gamma(k)^T\,\boldsymbol{\mathcal{W}}(p)^T\,\xi$ *QP and constraints*
$\text{s.t.} \quad G_\emptyset(k)\,\xi \leq W_\emptyset(k)\,\Gamma(k) + \mathcal{S}_\emptyset(k)$

14) $\xi^* \rightarrow \Delta U(k)$ *the incremented vector for the control signal*

15) $U(k) = U(k-1) + \Delta U(k)$; *optimal solution for input control signal*

Output: Only the first element of the predicted control signal $U(k)$ applied to the system

4.4 Simulation and Experiment

As aimed in this chapter, the proposed dc-dc buck-boost converter is designed based on the values of the parameters, which are illustrated in Table 4.1. The variety in the L, C, VG, and R parameters lead to create multiple system models, each model different than the others. Therefore, to cover this variety, these models implemented and linearized at the operating points associated with it, as it is computed in subsection 2.3. Thus, the system with such multiple models can hardly be controlled using a regular control scheme. Therefore, the AMPC, reg-MPC and G.S-PI are implemented to test their performances against such a system with parameters' uncertainties.

Table 4.1. Parameters Value for the Converter for simulation model

Parameters		Nominal Value	Variations
Input voltage	VG	5 V	-/+ 20%
Inductor	L	100 uH	-10/+ 90%
Inductor resistive	rL	0.1 Ω	0%
Capacitor	C	220 uF	-10/+ 90%
Capacitor resistive	rC	0.1 Ω	0%
Resistive Load	R	1 KΩ	-/+ 20%
Switching frequency	fs	25 kHz	0%
Duty cycle	d	calculated	0%
Sampling time	Ts	0.00004 sec	0%

Fig. 4.3a and b illustrate the closed loop system for the dc-dc buck-boost converter, which is a single-input and single-output (SISO) control system. The input control signal $\tilde{u} = \tilde{d}$ is the manipulated variable (MV) and the system output is the capacitor voltage VC which is a measured output (OU) signal. As mentioned above, the goal is to design linear control systems capable of handling the dc-dc converter with the parameters' uncertainties. The closed loop of reg-MPC is designed without the use of the LPV model and it is designed using the nominal plant model. But in the running time, the converter will be influenced by the change in the parameter's values. The AMPC controller is designed offline with a one system model at the initial condition values as we did in the reg-MPC design. Then at the running time, the AMPC keeps updating its prediction model and calculating the objective cost function online using the information coming from the LPV model and the converter's feedback signal to match the changes in the system parameters. Both the reg-MPC and the AMPC are proposed to handle the inequality constraints applied to the input control signal U. The prediction horizon Np is varied to test their effectiveness on the system performance and outputs. The weighting matrices Q_x and R_u are valued as follow:

$$Q_x = \text{diag}[1, \dots, 1], \qquad R_u = \text{diag}[1, \dots, 1] \tag{4.14}$$

Also, the Gain Scheduling proportional and integral (G.S-PI) control system was considered to test its robustness and performance against the uncertainties of the parameters in the proposed dc-dc buck-boost converter. In the design of the G.S-PI controller, the lock-up tables were used to store the P and I gains that were calculated offline for every linearized model of the proposed dc-dc buck-boost converter. Fig. 4.3c shows the G.S-PI buck-boost converter's closed-loop control system structure using the

look-up tables. The result and outputs of this control system were compared with the implemented reg-MPC and AMPC control systems.

The projected reg-MPC, AMPC and G.S-PI for the proposed dc-dc buck-boost converter was simulated using the MATLAB and SIMULINK environment (version R-2020B) which are carried out on a laptop computer with CORE i7 1.8GHz CPU, 16 GB RAM, and a WINDOWS 10 professional operating system. This control system scheme was designed using the MPC, the AMPC, the lock-up table, the PID, and the LPV models in Simulink Toolboxes.

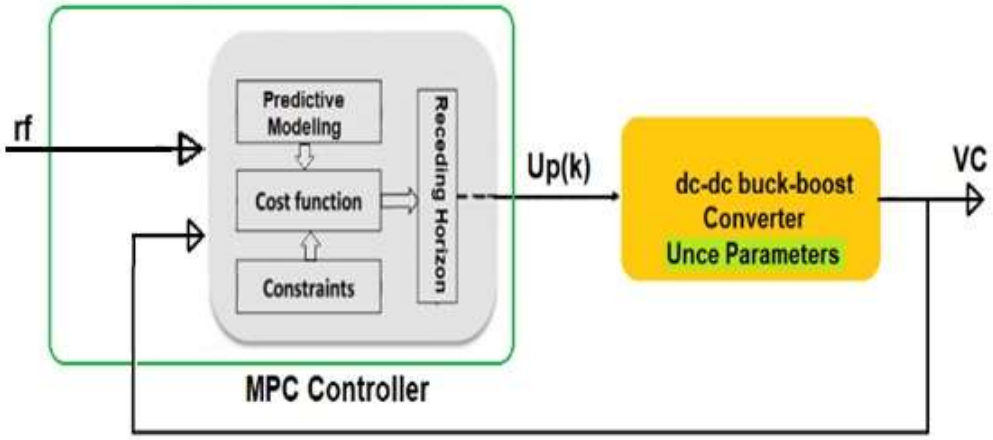

Fig 4.3(a). the reg-MPC for the dc-dc buck-boost converter control system.

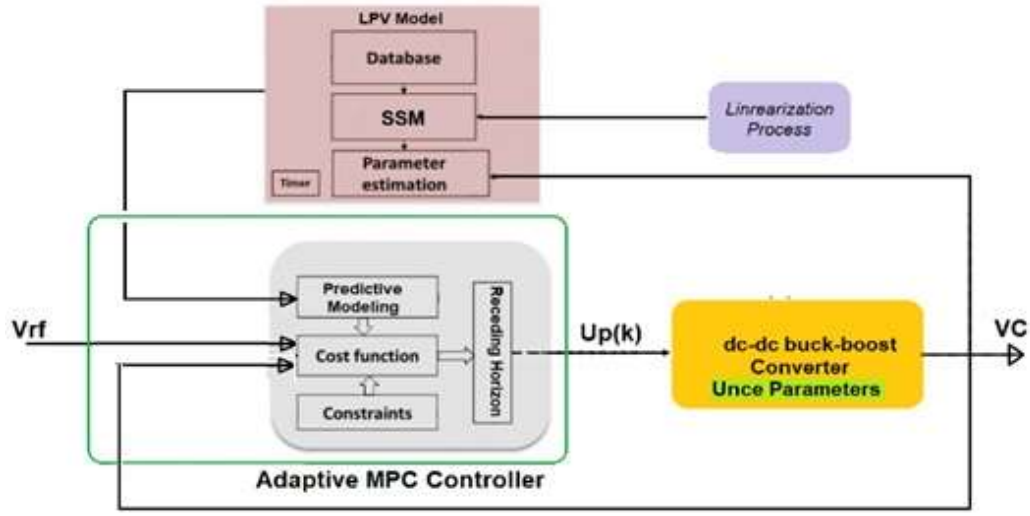

Fig 4.3(b). the AMPC and dc-dc buck-boost converter closed loop control system, including the LPV model

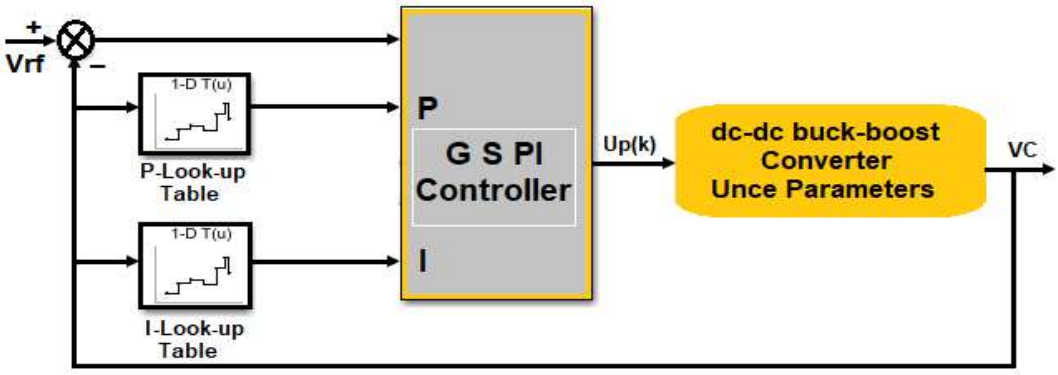

Fig 4.3(c). the G.S-PI and dc-dc buck-boost converter closed loop control system.

4.4.1 Simulation Analysis and Results

As it is proposed, the dc-dc buck-boost converter was implemented with parameters R, L, C and VG varied over time. Therefore, the three proposed control systems

were implemented to test their performance and robustness against these variants. Figure. 4.4 (X, Y, and Z) show the values of the input voltage VG in a range between minimum 4.27V and maximum 5.89V, a resistive load R minimum value of 0.994 K Ohms and maximum value of 1.169 K Ohms, a inductor L ranged between 9.66e-5 H and maximum 147e-6 H, and a capacitor C valued between 234e-6 F to 401e-6 F.

Figures. 4.5 and 4.6 show the performance of the reg-MPC and the AMPC when the prediction horizon was valued at Np= 10 and Np =100 respectively, the control horizon Nc=3, and the weighting matrices Q_x and R_u are valued as in the equation (4.14). The G.S-PI controller's gains listed in the Table. 4.2.

Table 4.2. shows the calculated gains for the G.S-PI controller

Time	$0-0.3$	0.3-0.5	0.5-0.7	0.7-0.9	$0.9-1$
Kp	-1.25e-5	-1.31e-5	-1.43e-5	-1.80e-5	-1.86e-5
Ki	-0.625	-0.653	-0.716	-0.898	-0.931

Figures . 4.5a and 4.6d represent the targeted control systems' input control signal U and the applied constraints to the AMPC and the reg-MPC controllers. Figure. 4.5b shows the AMPC, and the reg-MPC controllers were easily guided the dc-dc converter output voltage very fast to track the reference signal (Vrf) with an overshoot percentage of 50% in the AMPC and 30% in the reg-MPC; however, the G.S-PI was performing butter with no overshooting but responding very slow to reach the desired output voltage

level, this is in the first time period from 0 to 0.3 sec. In the time period between 0.6 sec to 0.8 sec, although the converter parameters changed with high values, all the controllers performed well with a tiny percentage of steady state error. Fig. 4.5c shows the inductor current iL, which is considered an unmeasured output signal. Although it starts with some oscillations at each time period, they get to the stability quickly; this is the performance of the AMPC and the reg-MPC controllers. On the other hand, no oscillations in the inductor current iL performed by the G.S-PI control system. More details listed in the Table. 4.3.

Table 4.3. shows the output voltage VC percentage steady state error (E_{ss}), overshoot (O_S), and settling time (sT)

Time	0 to 0.3 sec			0.6 to 0.8 sec	
	E_{ss} %	O_S %	sT sec	E_{ss} %	O_S %
AMPC	0	50	0.008	0	0
reg-MPC	0	30	0.004	3	0
G.S-PI	0.5	0	0.1	2.5	0

The performance of the AMPC and reg-MPC changed because of the change in the predictions horizon value Np=100. There was no change in the G.S-PI controller performance since the same gains were used for the same parameters' values. In Fig. 4.6e, despite a slight overshooting of 3%, the AMPC was able to force the output voltage

VC to reach the steady-state condition at the desired value in a very fast time. Although the parameters' values in the proposed dc-dc converter are varied, the AMPC shows high flexibility to pick the suitable LTI array from the LPV model, which matches these changes in the converter's parameters each time. The same figure shows the reg-MPC performed poorly to track the reference signal Vrf. It performed with a high amount of a steady-state error about 25% in the period between 0 sec to 0.3 sec, and its performance became worse with the change in converter

parameters. Also, the performance of the G.S-PI controller is well, but in the period between 0.6 sec to 0.8, the output voltage has some steady-state error of 2.5%. More details can be found in TABLE. 4.4. Figure. 4.6f shows the inductor current, which is considered as an unmeasured output signal. Although it starts with some oscillations, it got stable quickly; this is in AMPC and reg-MPC controllers' performance, and no oscillations in the G.S-PI controller performance.

Table 4.4. shows the output voltage VC percentage steady state error (E_{ss}) overshoot *(*O_S*)* and settling time (sT)

Time	0 to 0.3 sec			0.6 to 0.8 sec	
	E_{ss} %	O_S %	sTsec	E_{ss} %	O_S %
AMPC	0	3	0.004	0	0
reg-MPC	25	0	0.004	27	0
G.S-PI	0.5	0	0.1	2.5	0

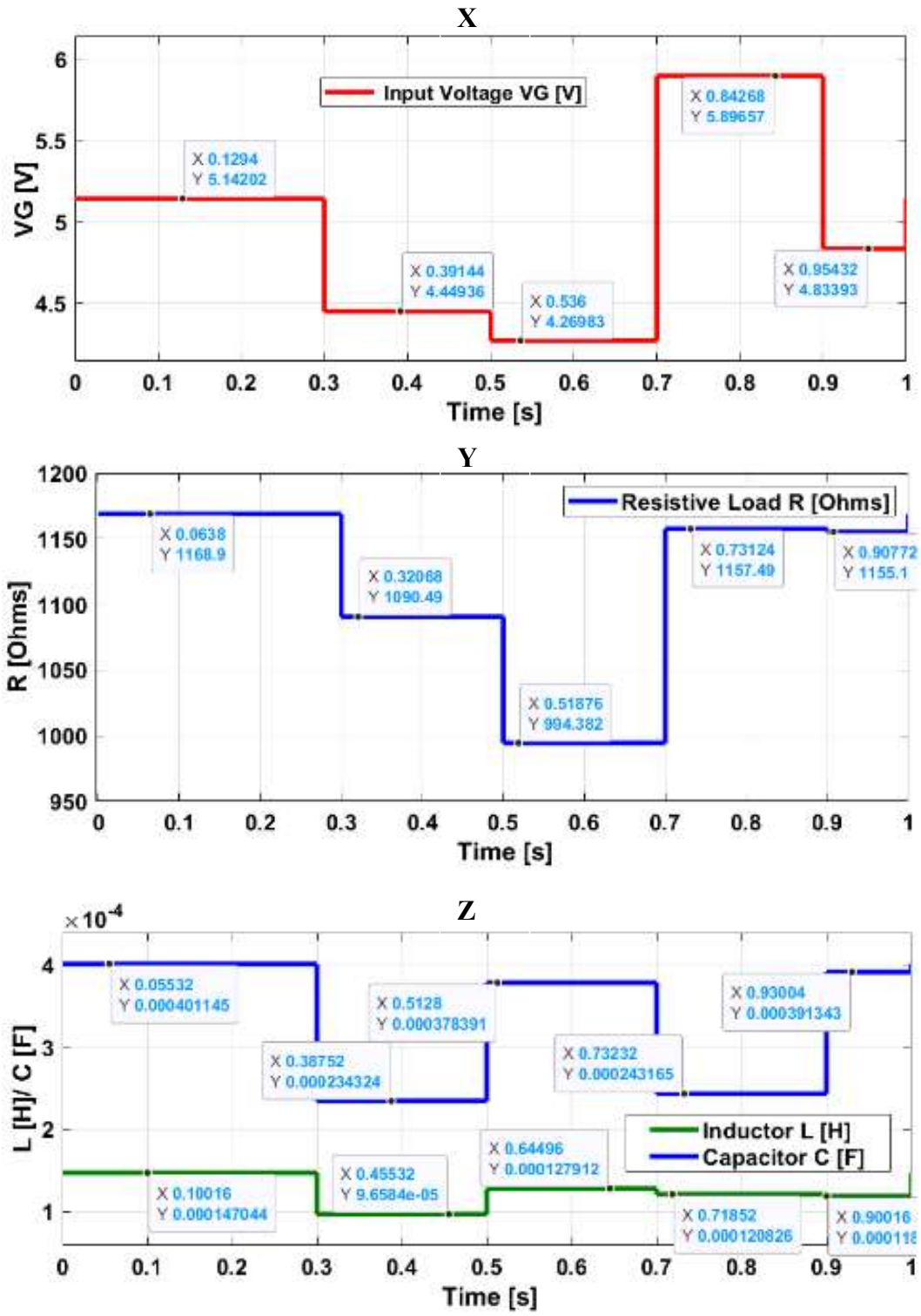

Fig 4.4 X) for the input voltage (VG), Y) for the resistive load (R) values, and Z) for the values of the inductor (L) and the capacitor (C)

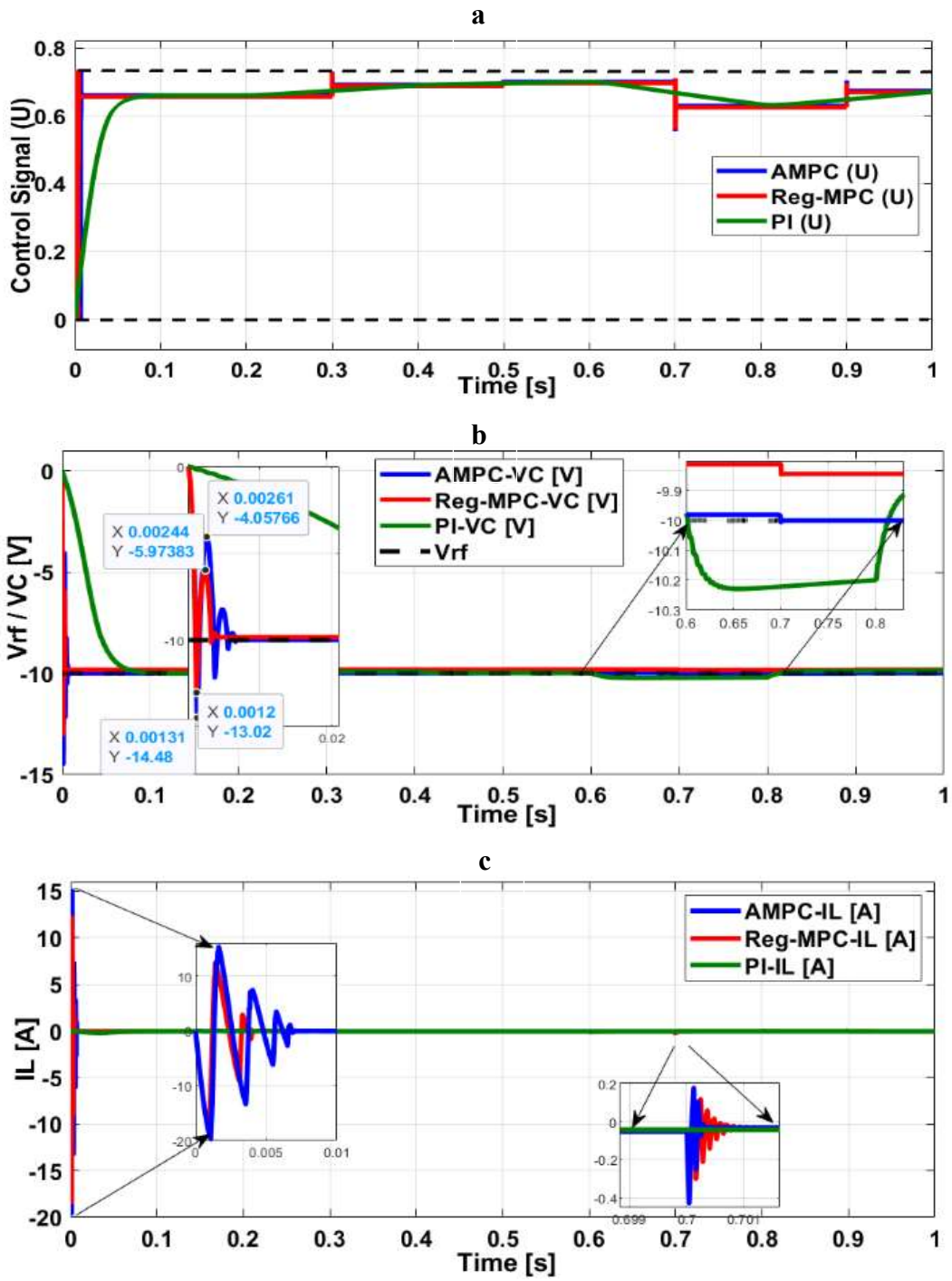

Fig 4.5 (a, b, and c) show the control signal (U), the reference voltage (Vrf), the closed loop system output voltage (VC), and the inductor current (iL) for all targeted control systems

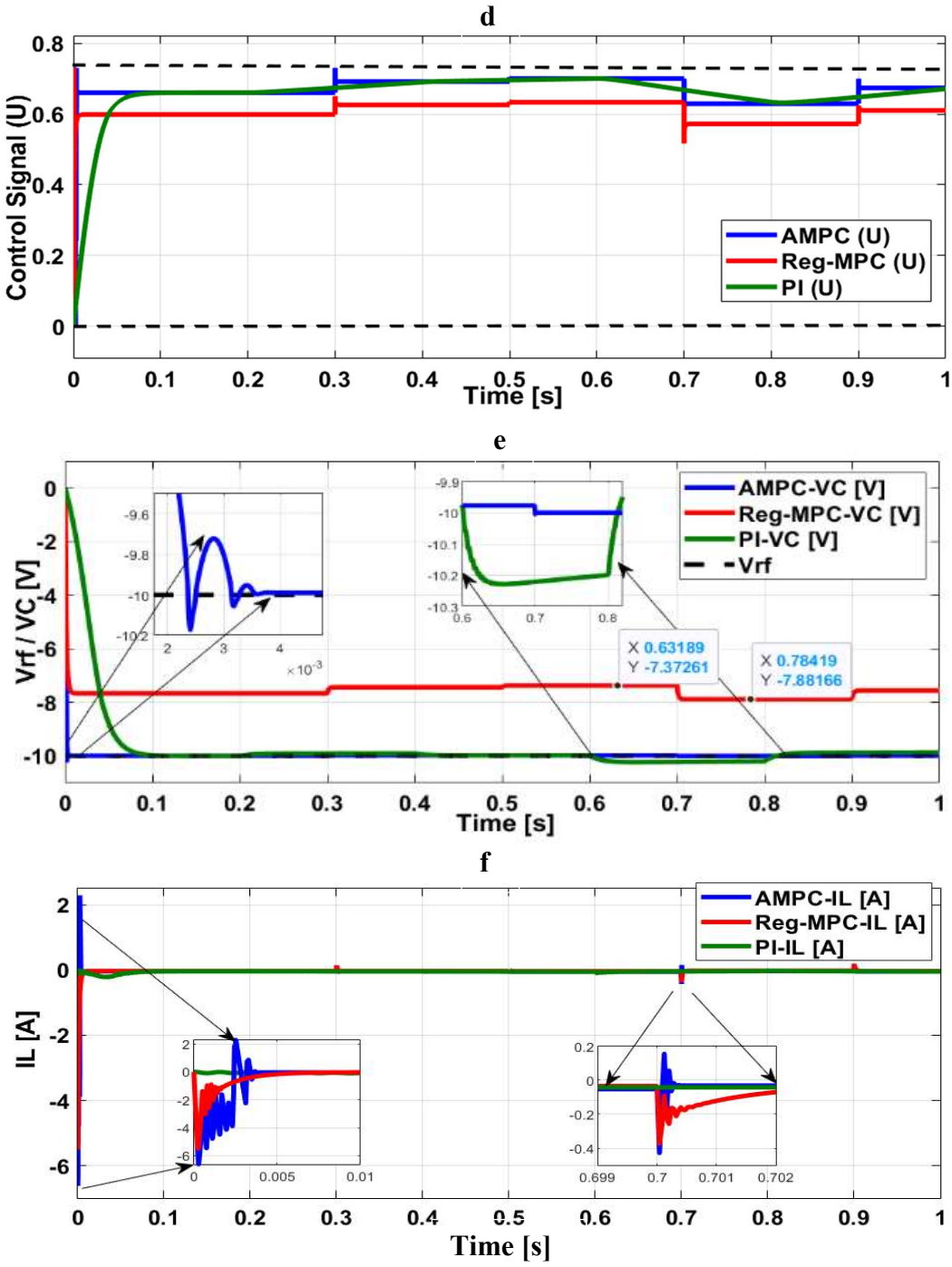

Fig 4.6 (d, e, and f) show the control signal (U), the reference voltage (Vrf), the closed loop system output voltage (VC), and the inductor current (iL) for all targeted control systems.

4.4.2 Comparison with Other Existing Control Approaches

In this sub-section, the proposed AMPC control system is compared with the offset free finite set MPC (OFFS-MPC) control algorithm [49] in terms of the steady state error, the percentage overshoot, and the settling time. Despite the OFFCS-MPC shows high robustness and performances in terms of the settling time around 2 ms, the percentage of the voltage overshooting less than 1%, and smoothly tracking the reference voltage signal with 0% steady state error percentage, the impacts of the value changes in the resistive load, the inductor, the capacitor, and the input voltage when they all happen at the same time have not been shown. On the other hand, although the proposed AMPC control scheme relatively has a slower response and higher voltage overshooting, its performance remains very well although all the system parameters, including the input voltage VG and the resistive load R have a high percentage of uncertainties applied at the same time. In terms of the inductor current iL, the OFFCS-MPC system obviously has no control over it. Therefore, the iL is highly impacted by the uncertainties in the system parameters. In contrast, although the inductor current iL is counted as an unmeasured output signal in the proposed AMPC control system, the stability in the output voltage VC positively affected the inductor current iL performance.

Also, the proposed AMPC control system was compared with some existing MPC control algorithms. The comparison was in the number of the iterations at different prediction horizons Np=10 to 30 increased by 10. The max-iteration was set to 1000, and the terminal tolerance was 0.001. the proposed AMPC control system compared with the online active set solver (qpOASES) algorithm [47], and the Accelerated Dual Gradient Projection (GPAD) algorithm [48] as detailed in the Table. 4.5.

Table 4.5. shows the number of iterations at different prediction horizons.

Algorithms	Np=10		Np=20		Np=30	
	Min	Max	M	Max	Min	Max
AMPC	1	8	1	7	1	7
qpOASES	2	12	11	20	21	35
GPAD	1	17	1	26	1	37

From Table. 4.5, the AMPC has the lowest numbers of the maximum iterations between 7 to 8 iterations. On the other hand, the compared control algorithms' iteration numbers increased as the prediction horizon Np was increased.

Another side of the comparison is in regards to the hardware cost, which was done with two of the MPC algorithms that exist in the literature. As mentioned above, the proposed AMPC control system was implemented in real-time using Arduino Mega 2560, which costs about $15 based on the price from the Amazon website [50]. In contrast, the algorithms in the references [25] and [49] were implemented on relatively high priced hardware systems. That concludes that the proposed AMPC optimization process does not require a heavy computation burden, which can be carried on a simple microprocessor such as the Arduino Mega 2560.

4.4.3 Real Time Experiment and Results

The AMPC and LPV control system for the dc-dc buck-boost converter was implemented and built on an Arduino Mega microcontroller, which is an ATmega 2560 CPU, with 54 digital input/output, 16 analog inputs. Also, it is provided with 256 bytes flash memory size for the code storage and CPU clock speed of 16MHZ. The proposed real time control system was coded and implemented using the MATLAB, SIMULINK 2020B and the ARDUINO support packages. Fig. 4.7 and 4.8 show the real-time closed loop control system and the toolboxes that were used to build the connectivity between the implemented Simulink model to the Arduino Mega and the real-time dc-dc buck-boost converter circuit.

There were four signals fed to the Simulink model from the external via the Arduino analog blocks and one signal sent to the dc-dc buck-boost converter through the Arduino PWM block. These signals are the feedback voltage, feedback current, reference voltage, input voltage, and the control signal U. The feedback voltage and current signals were measured and fed back from the converter. The reference voltage Vrf was measured and fed from a separate DC voltage source, and the input voltage signal came from a DC voltage source. The control signal U sent as a PWM signal to the dc-dc buck-boost converter as they can be seen in Fig. 4.7 and 4.8.

The dc-dc buck-boost circuit was built on a breadboard with components values, L = 100 uH for the inductor, the capacitor C=1000 uF, resistive load R= 0.9 to 1.2 K Ohm, and the input voltage VG=5 V DC. Since the Arduino cannot read the negative voltage values, an inverting operation amplifier (op-amp) was built to invert the proposed converter negative output voltage and fed to the Arduino using the ACS712 Module voltage and

current sensor. Figures.10-12 represent the output of the proposed AMPC for the dc-dc buck-boost converter closed-loop control system, measured by the oscilloscope over the channels numbered 1 and 2. Channel 1 (blue) is the output voltage, and channel 2 (purple) is the reference voltage signals. As shown in Figures. 10-12, the controller works very well to track the reference signal Vrf. In Figure. 10, the input voltage VG was set to 5V DC, and the reference signal was Vrf= 9.2V. The output voltage was fast in reaching the steady-state condition in about 3 sec and the rise time RT of 1.4 sec with some steady-state errors E_{ss} of approximately 11.9%. Also, the proposed control system robustness was tested against the sudden changes in the resistive load.

During the running time, the resistive load was changed from 0.9 to 1.2 K Ohms. The output was well maintained to be kept at the desired output; although the load was changed suddenly, the AMPC control system inquired about 1.9 sec to bring the output voltage signal back to the 7.16V as it can be seen in Fig. 4.10. The load in Fig. 4.11 was changed from 0.9K Ohms to 1K Ohm, and the control system was very well responded. It takes about 2.4 sec to bring the output back to the desired output voltage. The output voltage range was limited up to 10 volts maximum that was due to the op amp range which limited to 10 DC volt; however, the system without the op amp can go up to -25V DC.

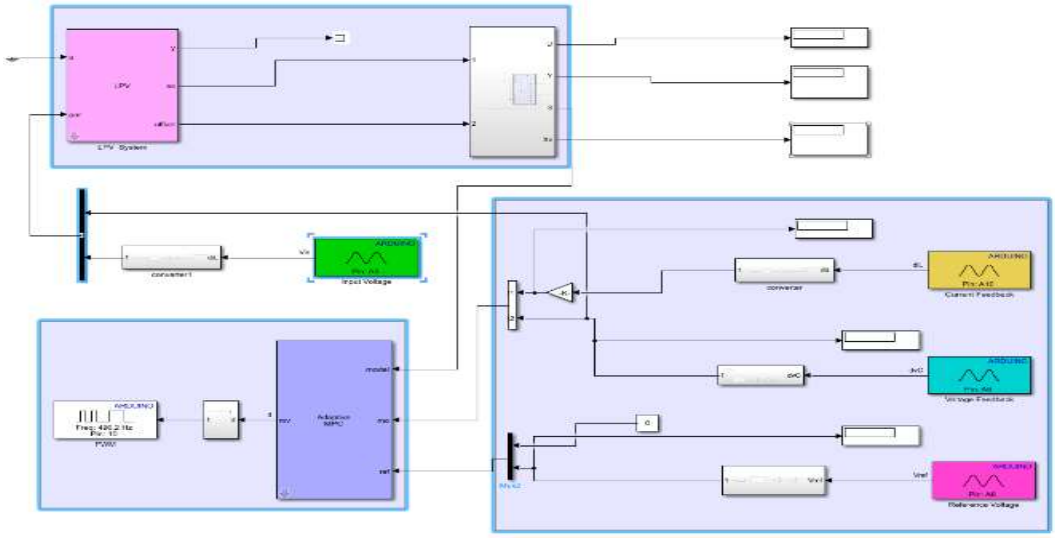

Fig 4.7. The Simulink model of the AMPC and LPV control system for the dc-dc buck-boost converter

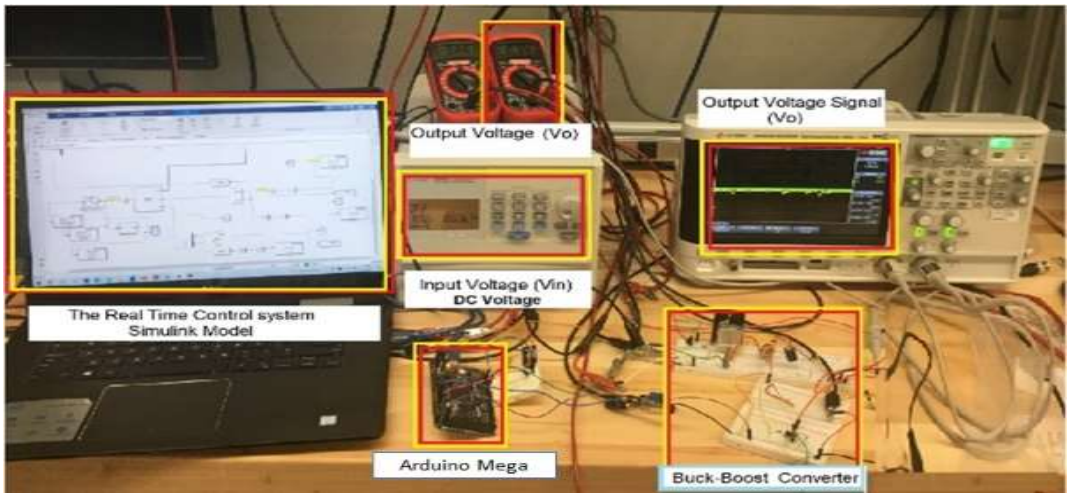

Fig 4.8. The Real time experiment for the closed loop AMPC and LPV for the dc-dc buck-boost converter

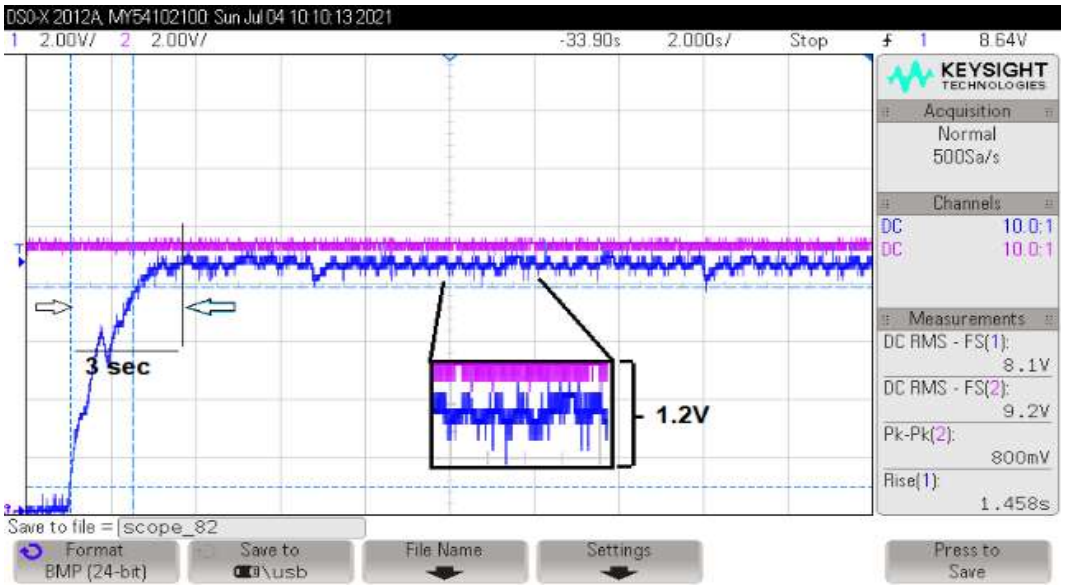

Fig 4.9. Shows the output voltage (VC=8.1V) when the Reference voltage (Vrf =9.2V), the Input voltage (Vin=5V) and Resistive load R=1k ohms

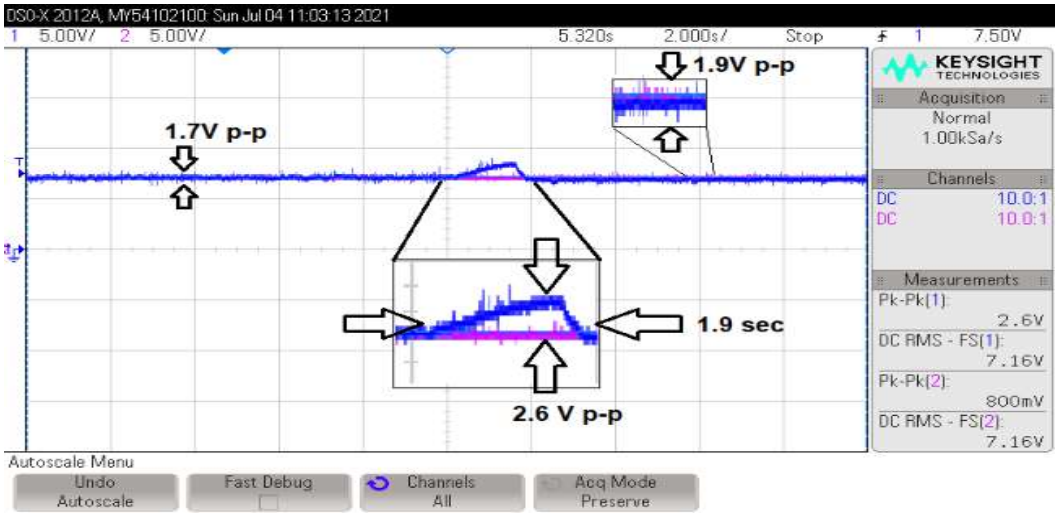

Fig 4.10. Shows the output voltage (VC=7.16V) when the Reference voltage (Vrf =7.16V), the Input voltage (Vin=5V) and Resistive load R=1k ohms to 1.2k Ohms

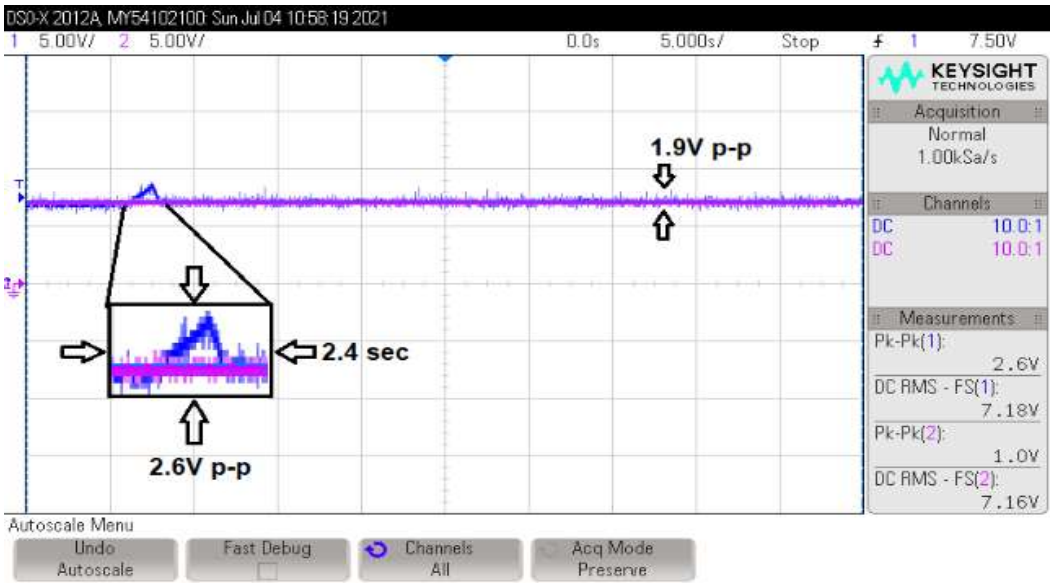

Fig 4.11. Shows the output voltage (VC=7.18V) when the Reference voltage (Vrf =7.16V), the Input voltage (Vin=5V) and Resistive load R=0.9k ohms to 1k Ohms.

4.5 CHAPTER CONCLUSION

In this chapter, the proposed AMPC-LPV control system was implemented to control the output voltage of a dc-dc buck-boost converter system model. The proposed system model was built out of parameters with not precisely known values; they were assumed with +/-20% uncertainties. Due to the switching behaviors and the parameters' uncertainties, this system was strongly nonlinear; thus, it needed a control system that could be updated to successfully carry out these changes in which the AMPC was the best control system used. Since the AMPC is a linear control system, the system was linearized multiple times at various operating conditions to create the LPV system. The implemented control system was tested in simulation and in real-time environments using

the MATLAB, Simulink software, and Arduino microcontroller. The proposed control system outputs were compared with different control system schemes. Also, the comparison was in regards to the computational time in which the proposed control system revealed higher performance against some of the existing control systems in the literate. The performance of the proposed system showed high quality to handle the system with a higher level of nonlinearity caused by the switching behaviors and the parameters' uncertainties.

CHAPTER. FIVE

CONCLUSION AND FUTURE WORK

5.1 The Conclusion

This dissertation investigated the implementation of the Model Predictive Control system in different approaches that could control the dc-dc power converter and the power industrial applications. In the first control approach, the implemented control system was designed with a discrete linear system of the proposed dc-dc buck-boost converter, where all of the system and the control system parameters are known and no noise or disturbances were added to the system. The goal of this control approach was to maintain a constant output voltage of the proposed dc-dc converter. Since the MPC control system is an optimization-based technique, the quadratic programming (QP) problem, which was subjected to linear inequality constraints, was proposed to minimize the error in the input control signal (U) which was iterated to reduce the error between the converter output and the desired reference signal r(k). It is evident from the result figures that the system performed very well in terms of the overshooting; it was only between 0.96% and 1.2% in the worst-case scenarios. Also, the converter worked as required in case of buck or boost operations, the simulation outputs showed the fast response of the system when the reference voltage was 60Vsame performance when the required output was 10V.

In the second case study of the control design, the proposed plant model of the dc-dc buck converter-driven dc-motor was mathematically calculated as a discrete-time linear MISO state-space system. The input signals of the proposed plant system were

considered as the input control signal (the manipulated input signal) and the dc motor load torque as an input disturbance (unmeasured disturbance), and the goal was to control the speed of the proposed dc motor even with the load torque disturbance. The same linear MPC approach was associated with a Kalman filter observer to assist the MPC control system estimate the system states when the load torque disturbance was added to the dc motor. Again, the optimization of the MPC control system was done by considering solving the QP problem subjected to an inequality constraint applied to the input control signal. The control system performance was tested at different values of the prediction horizon; also, the robustness of the control system design, with the assistant of the Kalman Filter Observer, was approved when different load torque values were added to the dc motor. The experimental results of the dc-dc buck converter driven dc-motor also approved that the dc-dc buck converter was highly successful in reducing the power consumption to derive. As shown in the figures, the proposed dc motor, the needed voltage, and current were about ~22 V and ~ 3.4A at the steady-state condition; this is when the highest load torque value was added.

In Chapter 4, the proposed control system was projected to control a system with higher level of the parameters uncertainties. The proposed dc-dc buck-boost converter was assumed that it supplied from an unsustainable input voltage source VG, and the other parameters the inductor L, the Capacitor C and the Resistive R were not precisely known but their values fluctuated in +/- 20% range of uncertainties. These uncertainties, and the dc-dc converter's original switching behaviors, made it act as a nonlinear system model. Therefore, a linear AMPC control scheme was applied to such a nonlinear system; the proposed plant model linearized at different operating conditions to create a set of

LTI models covering the proposed dc-dc converter working range. A discrete LPV model was then modeled as an array of state-space models representing this converter system's varying dynamics based on the scheduling parameters. For this reason, the AMPC was chosen because of its online optimization and the ability to update its prediction model based on the changes in the plant model and the operating conditions. The AMPC continues updating its predicted plant model and the operating conditions over a prediction horizon to maintain constant output values tracking the applied reference signal. The performance of proposed AMPC control approach was compared in terms of the performance with some of the existed MPC approaches [47]-[49]. Also, the proposed AMPC results and outputs were compared with the results of designed reg-MPC and G.S-PI control systems, which were modeled without using the LPV model. Then, the AMPC algorithm was implemented in real-time using an Arduino Mega 2560 microcontroller.

Finally, in summary, the linear MPC for linear power electronics and applications plant systems is a perfect control approach, even if the plant system is affected by any type of disturbance. Also, the proposed AMPC control algorithm highly performed in terms of the system outputs quality even if a system with uncertainties; its real-time optimization requires relatively low computational burden, and the used hardware is cheap in price, which can be simply implemented at a simple laboratory using MATLAB and Simulink built-in functions and toolboxes, and the Simulink Arduino support packages.

5.2 Future work

1. Implementing the MPC controller with different types of the QP optimization problems for higher order dc-dc power converters.

2. Implementing the AMPC-LPV control system for a MIMO plant model and build it in the real time environment such as the Field Programmable Gate Array (FPGA).

3. Implementing the AMPC-LPV to work with the renewable energy systems, such as the Solar Photo Voltic power system or the Wind Turbine Power system.

4. Consider modelling the dc-dc power converter in a nonlinear modeling including different types of the disturbances using the Nonlinear MPC control scheme.

REFERENCES

1. M. P. Kazmierkowski, R. Krishnan, F. Blaabjerg. ‘CONTROL IN POWER ELECTRONICS’, Academic Press, 2002

2. J. Rodriguez, Patricio Cortes, ‘PREDICTIVE CONTROL OF POWER CONVERTERS AND ELECTRICAL DRIVES’, Hohn Wiley & Sons, Ltd, 2012.

3. J.Rodriguez and P. Cortes, ‘Classical Control Methods for Power Converters and Drivers’, 2012, pp. 248

4. Nassim Khaled Bibin Pattel, “Practical Design and Application of Model Predictive Control”,1st Edition,MPC for MATLAB® and Simulink® Users, Paperback ISBN: 9780128139189 eBook ISBN: 9780128139196

5. L. Wang, “Model Predictive Control System Design and Implementation Using MATLAB”, School of Electrical and Computer Engineering, RMIT University Melbourne, VIC 3000 Australia ISBN 978-1-84882-330-3 e-ISBN 978-1-84882-331-0

6. S. Bououden, O. Hazil, S. Filali and M. Chadli, "Modelling and model predictive control of a DC-DC Boost converter," 2014 15th International Conference on Sciences and Techniques of Automatic Control and Computer Engineering (STA), Hammamet, 2014, pp. 643-648, doi: 10.1109/STA.2014.7086663

7. L. Cheng, P. Acuna, Ricardo P. Aguilera, J. Jiang, S. Wei, John E. Fletcher, Dylan D. C. Lu “Model Predictive Control for DC–DC Boost Converters with Reduced-Prediction Horizon and Constant Switching Frequency”, IEEE TRANSACTIONS ON POWER ELECTRONICS, VOL. 33, NO. 10, OCTOBER 2018

8. P. Karamanakos, T. Geyer and S. Manias, "Direct Voltage Control of DC–DC Boost Converters Using Enumeration-Based Model Predictive Control," in IEEE Transactions on Power Electronics, vol. 29, no. 2, pp. 968-978, Feb. 2014, doi: 10.1109/TPEL.2013.2256370.

9. L. Cheng, P. Acuna, Ricardo P. Aguilera, J. Jiang, S. Wei, John E. Fletcher, Dylan D. C. Lu “Model Predictive Control for DC–DC Boost Converters with Reduced-Prediction Horizon and Constant Switching Frequency”, IEEE TRANSACTIONS ON POWER ELECTRONICS, VOL. 33, NO. 10, OCTOBER 2018

10. P. Cáceres, C. Restrepo, C. R. Baier and J. Muñoz, "Finite control set model predictive current control of the Coupled-Inductor Buck–Boost DC–DC Switching Converter," 2018 IEEE International Conference on Automation/XXIII Congress of the Chilean Association of Automatic Control (ICA-ACCA), 2018, pp. 1-6, doi: 10.1109/ICA-ACCA.2018.8609723

11. Q. Xu, Y. Yan, C. Zhang, T. Dragicevic and F. Blaabjerg, "An Offset-Free Composite Model Predictive Control Strategy for DC/DC Buck Converter Feeding Constant Power Loads," in IEEE Transactions on Power Electronics, vol. 35, no. 5, pp. 5331-5342, May 2020, doi: 10.1109/TPEL.2019.2941714.

12. C. Vlad, P. Rodriguez-Ayerbe, E. Godoy, and P. Lefranc, ‘‘Advanced control laws of DC–DC converters based on piecewise affine modelling. Application to a stepdown converter,’’ IET Power Electron., vol. 7, no. 6, pp. 1482–1498, 2014.

13. T. Geyer, G. Papafotiou, and M. Morari, ‘‘Hybrid model predictive control of the step-down DC–DC converter,’’ IEEE Trans. Control Syst. Technol., vol. 16, no. 6, pp. 1112–1124, Nov. 2008.

14. W. Tu, G. Luo, Z. Chen, C. Liu and L. Cui, "FPGA Implementation of Predictive Cascaded Speed and Current Control of PMSM Drives With Two-Time-Scale Optimization," in IEEE Transactions on Industrial Informatics, vol. 15, no. 9, pp. 5276-5288, Sept. 2019, doi: 10.1109/TII.2019.2897074.

15. R. C. B. Rego, "LPV Modeling of Boost Converter and Gain Scheduling MPC Control," 2019 IEEE 15th Brazilian Power Electronics Conference and 5th IEEE Southern Power Electronics Conference (COBEP/SPEC), 2019, pp. 1-5, doi: 10.1109/COBEP/SPEC44138.2019.9065825

16. B Jee-Hun Park, Tae-Hyoung Kim, Toshiharu Sugie, “Output feedback model predictive control for LPV systems based on quasi-min–max algorithm”,Automatica, Volume 47, Issue 9, 2011,
    Pages 2052-2058, ISSN 0005-1098,
    https://doi.org/10.1016/j.automatica.2011.06.015.

17. T. Kim, J. Park and T. Sugie, "Output-feedback Model Predictive Control for LPV Systems with Input Saturation based on Quasi-Min-Max Algorithm," Proceedings of the 45th IEEE Conference on Decision and Control, 2006, pp. 1454-1459, doi: 10.1109/CDC.2006.377038

18. Cavanini, L., Ippoliti, G. & Camacho, E.F. Model Predictive Control for a Linear Parameter Varying Model of an UAV. J Intell Robot Syst 101, 57 (2021). https://doi.org/10.1007/s10846-021-01337-x

19. B. Zhu, Z. Zheng and X. Xia, " Constrained Adaptive Model-Predictive Control for a Class of Discrete-Time Linear Systems With Parametric Uncertainties," in IEEE Transactions on Automatic Control, vol. 65, no. 5, pp. 2223-2229, May 2020, doi: 10.1109/TAC.2019.2939659.

20. T.Hausberger, A.Kugi, A.Eder, W.Kemmetmüller "High-speed nonlinear model predictive control of an interleaved switching DC/DC-converter", Viktor Bro and Alexander Medvedev Control Engineering Practice • October 2020

21. F. Asadi, S. Pongswatd, K. Eguchi, N. L. Trung, ,"Modeling Uncertainties in DC-DC Converters with MATLAB® and PLECS" ISBN: 9781681734385 ebook, DOI 10.2200/S00875ED1V01Y201809EEL006

22. M. Modabbernia, F. K. Khoshkbijari, R. Fouladi, S. S. Nejati "The State Space Average Model of Buck- Boost Switching Regulator Including all of The System Uncertainties" International Journal on Computer Science and Engineering (IJCSE).

23. M. E. Albira, A. Alzahrani and M. Zohdy, "Model Predictive Control of DC-DC Buck-Boost Converter with Various Resistive Load Values," 2020 Global Congress on Electrical Engineering (GC-ElecEng), Valencia, Spain, 2020, pp. 124-128, doi: 10.23919/GC-ElecEng48342.2020.9285986.

24. Erickson, Robert W., Maksimovic, Dragan, "Fundamentals of Power Electronics". ISBN:978-0-306-48048-5. https://www.springer.com/gp/book/9781475705591#aboutBook,

25. Z. Liu, L. Xie, A. Bemporad and S. Lu, "Fast Linear Parameter Varying Model Predictive Control of Buck DC-DC Converters Based on FPGA," in IEEE Access, vol. 6, pp. 52434-52446, 2018, doi: 10.1109/ACCESS.2018.2869043.

26. C. Restrepo, J. Calvente, A. Cid-Pastor, A. E. Aroudi and R. Giral, "A Noninverting Buck–Boost DC–DC Switching Converter With High Efficiency and Wide Bandwidth," in IEEE Transactions on Power Electronics, vol. 26, no. 9, pp. 2490-2503, Sept. 2011, doi: 10.1109/TPEL.2011.2108668

27. M. E. Albira, A. Alzahrani and M. Zohdy, "Model Predictive Speed Control of DC-DC Buck Converter Driven DC-motor with Various Load Torque Values," 2020 IEEE International IOT, Electronics and Mechatronics Conference (IEMTRONICS), Vancouver, BC, Canada, 2020, pp. 1-6, doi: 10.1109/IEMTRONICS51293.2020.9216459.

28. J. Yang, H. Wu, L. Hu, S.Li, "Robust Predictive Speed Regulation of Converter-Driven DC Motors via a Discrete-Time Reduced-Order GPIO", IEEE TRANSACTIONS ON INDUSTRIAL ELECTRONICS,VOL.66,NO.10, OCT 2019

29. M.A. Ahmad, R.M.T. Raja Ismail, M.S. Ramli," Control Strategy of Buck Converter Driven Dc Motor: a Comparative Assessment", Australian Journal of Basic and Applied Sciences, 4(10): ISS 1991- 8178

30. J.Linares-Flores, J. Reger, and H. Sira-Ram´ırez "Speed-sensorless tracking control of a DC-motor via a double Buck-converter", Proceedings of the 45th IEEE Conference on Decision & Control Manchester Grand Hyatt Hotel San Diego, CA, USA, December 13- 15, 2006

31. T. K. Roy, M. F. Pervej, F. K. Tumpa, and L. C. Paul, "Nonlinear Adaptive Controller Design for Velocity Control of a DC Motor Driven by a DC-DC Buck Converter Using Backstepping Ap", 2nd International Conference on Electrical, Computer & Telecommunication Engineering (ICECTE)8-10 December 2016, Rajshahi-6204, Bangladesh

32. Ramon Silva-Ortigoza, Victor Manuel Hern ´ andez-Guzm ´ an, Mayra Antonio-Cruz, and Daniel Mu ´ noz-Carrillo, "DC/DC Buck Power Converter as a Smooth Starter for a DC Motor Based on a Hierarchical Control", IEEE TRANSACTIONS ON POWER ELECTRONICS, VOL. 30, NO. 2, FEBRUARY 2015

33. F. E. H. Velasco, J. E. Candelo-Becerra, A. R. Santamaría, "Dynamic Analysis of a Permanent Magnet DC Motor Using a Buck Converter Controlled by ZAD-FPIC"

34. L.Wang, S. Chai, D. Yoo, L. Gan, K. Ng, "PID and Predictive Control of Electrical Drives and Power Converters Using MATLAB/Simulink", published 2015 john wiley & sons singaphore pte. Ltd, (ISBN: 9781118339442)

35. J. M. MacIejowski "Predictive Control with Constraints 1st Edition". Prentice Hall, Harlow, 1st edition, 2002

36. Kouvaritakis, B. and Cannon, M. Model Predictive Control: Classical, Robust and Stochastic. Springer, 2015, (ISBN-13: 978-3319248516), (ISBN-10: 3319248510).

37. K. Gaouzi, H. El Fadil, A. Rachid, F. Z. Belhaj and F. Giri, "Constrained model predictive control for dc-dc buck power converters," 2017 International Conference on Electrical and Information Technologies (ICEIT), Rabat, 2017, pp. 1-5, doi: 10.1109/EITech.2017.8255245

38. The MathWorks. (2021). Adaptive MPC. [Online]. Available: https://www.mathworks.com/help/mpc/ug/adaptive-mpc.html?s_tid=srchtitle

39. https://en.wikipedia.org/wiki/Model_predictive_control

40. www. books.google.com/ngrams

41. M. E. Albira and M. A. Zohdy, "Adaptive Model Predictive Control for DC-DC Power Converters With Parameters' Uncertainties," in IEEE Access, vol. 9, pp. 135121-135131, 2021, doi: 10.1109/ACCESS.2021.3113299.

42. The MathWorks. (2021). LPV modeling. [Online]. Available: https://www.mathworks.com/help/control/ug/linear-parameter-varying-models.html#bukg8gc-1

43. L. Cavanini, G. Ippoliti, and E. F. Camacho, ''Model predictive control for a linear parameter varying model of an UAV,'' J. Intell. Robotic Syst., vol. 101, p. 57, Mar. 2021, doi: 10.1007/s10846-021-01337-x

44. P. Falcone, M. Tufo, F. Borrelli, J. Asgari, and H. E. Tseng, ''A linear time varying model predictive control approach to the integrated vehicle dynamics control problem in autonomous systems,'' in Proc. 46th IEEE Conf. Decis. Control, New Orleans, LA, USA, Dec. 2007, pp. 2980–2985, doi: 10.1109/CDC.2007.4434137.

45. A. Bemporad. Model Predictive Control Linear Time-Varying and Nonlinear MPC. Accessed: May 2021. [Online]. Available: http://cse.lab.imtlucca.it/~bemporad/teaching/mpc/imt/2-ltv_nl_mpc.pdf

46. F. Borrelli, A. Bemporad, and M. Morari, Predictive Control for Linear and Hybrid Systems. Cambridge, U.K.: Cambridge Univ. Press, 2017, doi: 10.1017/9781139061759.

47. H. J. Ferreau, C. Kirches, A. Potschka, H. G. Bock, and M. Diehl, ‘‘qpOASES: A parametric active-set algorithm for quadratic programming,’’ Math. Program. Comput., vol. 6, no. 4, pp. 327–363, 2014.
48. P. Patrinos and A. Bemporad, ‘‘An accelerated dual gradient-projection algorithm for embedded linear model predictive control,’’ IEEE Trans. Autom. Control, vol. 59, no. 1, pp. 18–33, Jan. 2014

49. Q. Xu, Y. Yan, C. Zhang, T. Dragicevic, and F. Blaabjerg, ‘‘An offset-free composite model predictive control strategy for DC/DC buck converter feeding constant power loads,’’ IEEE Trans. Power Electron., vol. 35, no. 5, pp. 5331–5342, May 2020, doi: 10.1109/TPEL.2019.2941714.

50. Amazon.com. (2021). SunFounder Mega 2560 R3 ATmega2560-16AU Board Compatible With Arduino. [Online]. Available: https://www.amazon.com/SunFounder-ATmega2560-16AU-Board-CompatibleArduino/dp/B00D9NA4CY/ref=asc_df_B00D9NA4CY/?tag=hyprod20&linkCode=df0&hvadid=309773039951&hvpos=&hvnetw=g&hvrand=4955456828333502132&hvpone=&hvptwo=&hvqmt=&hvdev=c&hvdvcmdl=&hvlocint=&hvlocphy=9016965&hvtargid=pla599566677804&th=1

51. A. Bemporad, "Model Predictive Control Design: New Trends and Tools," Proceedings of the 45th IEEE Conference on Decision and Control, 2006, pp. 6678-6683, doi: 10.1109/CDC.2006.377490.

52. Zuhua Xu, Jun Zhao, Jixin Qian, and Yucai Zhu, “Nonlinear MPC using an Identified LPV Model”, *Industrial & Engineering Chemistry Research* 2009 *48* (6), 3043-3051,DOI: 10.1021/ie801057q

53. Predictive control with constraints, J.M. Maciejowski; Pearson Education Limited, Prentice Hall, London, 2002, pp. IX+331, price 35.99, ISBN 0-201-39823-0

PUPLISHED WORK

1. M. E. Albira, A. Alzahrani and M. Zohdy, "Model Predictive Speed Control of DC-DC Buck Converter Driven DC-motor with Various Load Torque Values," 2020 IEEE International IOT, Electronics and Mechatronics Conference (IEMTRONICS), 2020, pp. 1-6, doi: 10.1109/IEMTRONICS51293.2020.9216459.

2. M. E. Albira, A. Alzahrani and M. Zohdy, "Model Predictive Control of DC-DC Buck-Boost Converter with Various Resistive Load Values," 2020 Global Congress on Electrical Engineering (GC-ElecEng), 2020, pp. 124-128, doi: 10.23919/GC-ElecEng48342.2020.9285986.

3. M. E. Albira and M. A. Zohdy, "Adaptive Model Predictive Control for DC-DC Power Converters With Parameters' Uncertainties," in IEEE Access, vol. 9, pp. 135121-135131, 2021, doi: 10.1109/ACCESS.2021.3113299.